Marine and Petroleum Geology 181 (2025) 107493

Contents lists available at ScienceDirect

Marine and Petroleum Geology

journal homepage: www.elsevier.com/locate/marpetgeo

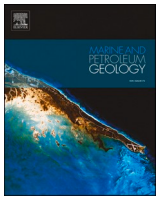

Characterization of the Miocene Castellón Sandstones Formation in the Western Mediterranean as a potential geological carbon storage site

Marc Gil-Ortiz [a,b,*], Enrique Gomez-Rivas [a,b], Juan Alcalde [c], Patricia Cabello [b,d], Luis Miguel Yeste [e], Gonzalo Zamora [f], Ángel Carrasco [f], David García Fernández-Valderrama [f], Antonio Martín-Monge [f], Marta Mañas [f], María Victoria Olgado Azpiazu [f], Manuel Ron Martín [f], Pujianto Lukito [f], Francisco Pángaro [f]

[a] Departament de Mineralogia, Petrologia i Geologia Aplicada, Facultat de Ciències de la Terra, Universitat de Barcelona, c/Martí i Franquès s/n, 08028, Barcelona, Spain
[b] Institut UB-Geomodels, Facultat de Ciències de la Terra, Universitat de Barcelona, c/Martí i Franquès s/n, 08028, Barcelona, Spain
[c] Geosciences Barcelona (GEO3BCN), CSIC, c/Lluís Solé i Sabarís s/n, 08028, Barcelona, Spain
[d] Departament de Dinàmica de la Terra i de l'Oceà, Facultat de Ciències de la Terra, Universitat de Barcelona, c/Martí i Franquès s/n, 08028, Barcelona, Spain
[e] Sedimentary Reservoirs Workgroup (SEDREGROUP), Departamento de Estratigrafía y Paleontología, Facultad de Ciencias, Universidad de Granada, av. Fuentenueva s/n, 18002, Granada, Spain
[f] Repsol Exploración S.A., Calle Méndez Álvaro, 44, 28045, Madrid, Spain

ARTICLE INFO

Keywords:
Sedimentology
Fluvial delta
Western Mediterranean
Seismic interpretation
Carbon capture and storage
Energy transition

ABSTRACT

In response to the growing interest in decarbonizing Europe's industrial hubs, this study examines the potential of the Miocene Castellón Sandstones Formation in the Valencia Trough for geological carbon storage. The proposed storage unit is represented by a siliciclastic succession formed mainly by sandstones and sandy heterolithics, in the Ebro Delta offshore area of the Valencia Trough. The sedimentological characterization of this succession, based on the study of a cored section from Amposta Marino C-2 well, has allowed to identify up to eleven lithofacies, comprising sandstones, heterolithics, calcarenites and carbonate breccias. These lithofacies can be grouped in six facies associations, including: 1) fluvial channel, 2) delta front proximal mouth bar, 3) delta front distal mouth bar, 4) proximal prodelta, 5) distal prodelta and 6) shelfal lag. The seismic stratigraphic analysis carried out throughout the study area points out to the additional presence of delta plain deposits in the northeastern sector of the study area, approximately at 30 km from the present-day Ebro delta shoreline. Based on the interpretation of these facies and seismic facies associations, the proposed depositional model consists of a river dominated, wave-influenced delta for the proto-Ebro deltaic system during the Late Miocene in the Valencia Trough. This study proposes that this sand-prone succession is presented as a good candidate for geological carbon storage in the study area, considering its proximity to the onshore Tarragona's industrial complex and its optimal reservoir characteristics. Additionally, the thick succession of the Ebro Shales also shows great potential as a vertical and lateral seal of the underlying Castellón Sandstones Formation.

1. From hydrocarbon exploration and production to geological carbon storage in the Valencia Trough

The current knowledge of the offshore subsurface reservoirs in the Valencia Trough (Fig. 1) has largely been developed by energy companies, which have historically focused on pursuing new oil and gas discoveries in the area.

Petroleum exploration in the Valencia Trough started in the late 1960s (Navarro Comet, 2019). A consortium led by Shell found the Amposta oil field in 1970, being the first oil discovery in the area (Figs. 1 and 2).

The main target of these wells was the fractured and karstified Mesozoic carbonates, proving the presence of effective petroleum systems mainly sourced by the Jurassic Ascla or Mas d'Ascla Formation

* Corresponding author. Departament de Mineralogia, Petrologia i Geologia Aplicada, Facultat de Ciències de la Terra, Universitat de Barcelona, c/Martí i Franquès s/n, 08028, Barcelona, Spain.
E-mail address: marc.gilortiz@ub.edu (M. Gil-Ortiz).

https://doi.org/10.1016/j.marpetgeo.2025.107493
Received 27 November 2024; Received in revised form 19 May 2025; Accepted 29 May 2025
Available online 31 May 2025

(Fig. 3) (Upper Kimmeridgian – Lower Titonian; Salas, 1989; Permanyer et al., 1999; Rossi et al., 2001; Salas and Permanyer, 2003; Playà et al., 2010) and the Lower Miocene Alcanar Formation (Di Cuia et al., 2017). The regional seal is constituted by the Middle Miocene Castellón Shales Formation (Fig. 3). Shallower successions in the overburden were in general not prospective, with the exception of the Tarraco structure in the basal Lower Miocene carbonates, the Dorada discovery in the basal Lower Miocene conglomerates and fractured dolostones (Aquitanian?; Clavell, 1992).

The vast knowledge acquired by the industry in the area and the interest of these energy companies and other public entities in decarbonizing industrial hubs in Europe (IEA, 2024) has recently led to the applications for investigation permits in the region with the aim of identifying strategic sites (Alcalde et al., 2021; Sun et al., 2021; Bullock et al., 2023) for the secure storage of large amounts of carbon dioxide in the subsurface. One of these research projects is framed in the TarraCO2 investigation permit (Martín-Monge et al., 2024) in the offshore area of the Ebro delta in the Valencia Trough, where this study is focused (Fig. 1). This permit request is located 50 km from the nearshore Tarragona's industrial area, a potential hub considered for decarbonization with CCS (Fernández-Canteli Álvarez et al., 2023) (Fig. 1).

The Valencia Trough infill (Fig. 3) presents a high potential for geological carbon storage in the subsurface by means of several sand-rich delta complexes. One of these successions is the Castellón Sandstones Formation, a poorly documented unit in academia with a challenging stratigraphic lateral correlation due to the paleorelief created by the Messinian Erosive Surface (MES) during the Late Miocene (Fig. 4) (Stampfli and Höcker, 1989; Escutia and Maldonado, 1992; Garcia--Castellanos et al., 2003; Frey-Martínez et al., 2004; Maillard et al., 2006; García et al., 2011; Lofi et al., 2011; Maillard and Mauffret, 2006; García-Castellanos and Villaseñor, 2011; Arche et al., 2010; Martínez del Olmo, 2011; Urgeles et al., 2011; Cameselle et al., 2014; Tassy et al., 2014; Martínez del Olmo and Martín, 2016; Martínez del Olmo, 2019; Pellen et al., 2019). Such formation forms part of the overburden of the prospective hydrocarbon fields in the area that were recently abandoned.

Transitional marginal to shallow marine delta complex deposits have been proved as excellent reservoirs for permanent geological carbon and storage elsewhere (Chadwick et al., 2004; Zweigel et al., 2004; Ambrose et al., 2008; Pham et al., 2013; Issautier et al., 2014, 2016; Gershenzon et al., 2015, 2017; Al-Khdheeawi et al., 2017, 2018; Soltanian et al., 2019; Eigbe et al., 2023), and accordingly, similar sedimentary units in the Valencia Trough present strong potential for geological carbon storage.

In this framework, this study presents a systematic stratigraphic and sedimentological analysis of the deltaic Castellón Sandstones Formation (Fig. 3), for their potential use as a carbon storage site. This is achieved by describing a continuous core section from Amposta Marino C-2 well, allowing to characterize these deposits in terms of correlatable facies associations, sedimentary model and reservoir quality properties of this unit. Additionally, seismic facies analysis in the area also aims to provide insightful knowledge further to the north-east from the location of this well.

2. Geological setting

The western margin of the Mediterranean is characterized by a series of basins opening from the Iberian eastern margin up to the western coasts of Corsica and Sardinia (Fig. 1). Among them, the Valencia Trough represents the southwestern extension of the Liguro-Provençal Basin and the main depocenter of the Ebro River sedimentation infill since the Middle Miocene.

The geomorphology of the Valencia Trough is defined by a NE-SW-trending basin bounded to the southeast by the Balearic Promontory and to the northwest by the Catalan Coastal Ranges and the Iberian continental margin (Fig. 1). The Valencia Trough formed on the stretched continental crust extending between the northeastern margin of the Iberian Plate and the Balearic Promontory (Fig. 2-A), corresponding to the northeastern extension of the Betic thrust belt (Roca and Guimerà, 1992). It has been interpreted as an aborted Late Oligocene – Early Miocene rift (Maillard et al., 1992; Álvarez-de-Buergo and Meléndez-Hevia, 1994) triggered by a back-arc extension in the upper Iberian plate. The retreat of the subducting Tethyan oceanic slab towards the SE promoted the formation of the Valencia Trough, and also the Liguro-Provençal and the Algerian basins (Roca et al., 1999, 2004; Ayala et al., 2015; Fang et al., 2021). The extension of the Iberian continental margin, including the Valencia Trough, was controlled by major seaward-dipping listric faults (Fig. 2-B) resulted from tectonic inversion of older Paleogene reverse faults of the Catalan Coastal Ranges (Sàbat et al., 1997; Roca et al., 1999).

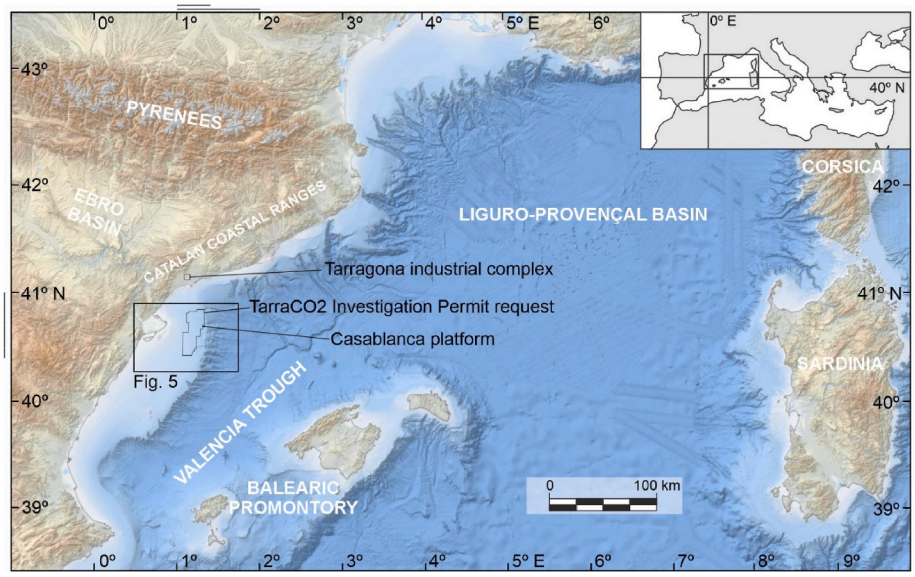

Fig. 1. Geographic location of the Ebro basin drainage system, the main geological domains of the northeastern Iberian Peninsula and Balearic Promontory, and location of the study area (Fig. 5) as part of the Valencia Trough in connection with the Liguro-Provençal basin. See also the location of the TarraCO2 Investigation Permit request in the area of study. Source basemap from EMODnet bathymetry portal (2024).

Syn-rift sedimentation initiated in the Valencia Trough during the Early Miocene (Alcanar Group, Figs. 3 and 4; Clavell and Berastegui, 1991; Clavell, 1992) under restricted marine conditions in a predominantly starved basin (Álvarez-de-Buergo and Meléndez-Hevia, 1994).

From the Middle Miocene, the post-rift sedimentation evolved into a prograding continental shelf that resulted in the deposition on the Ebro margin (Fig. 2-B), and corresponds to the onset of the proto-Ebro delta sedimentation (Fig. 4). This post-rift infilling is characterized by two main prograding megasequences separated by the Messinian Erosive Surface (MES), also referred as Messinian unconformity (Fig. 3). The first megasequence, also called the Castellón Group (Figs. 3 and 4), which is interpreted to have been developed from the Langhian to the Messinian, with an original thickness of ca. 1000 m (Soler et al., 1983; Lanaja, 1987; Martínez del Olmo, 1996; Evans and Arche, 2002; Cameselle and Urgeles, 2015). The deposition of the second megasequence, called Ebro Group (Figs. 3 and 4), started during the Zanclean (Zanclean flood; Garcia-Castellanos et al., 2009) and continues until the present day (Garcia- Sineriz et al., 1978; Soler et al., 1983; Clavell and Berastegui, 1991; Bertoni and Cartwright, 2005; Kertznus and Kneller, 2009).

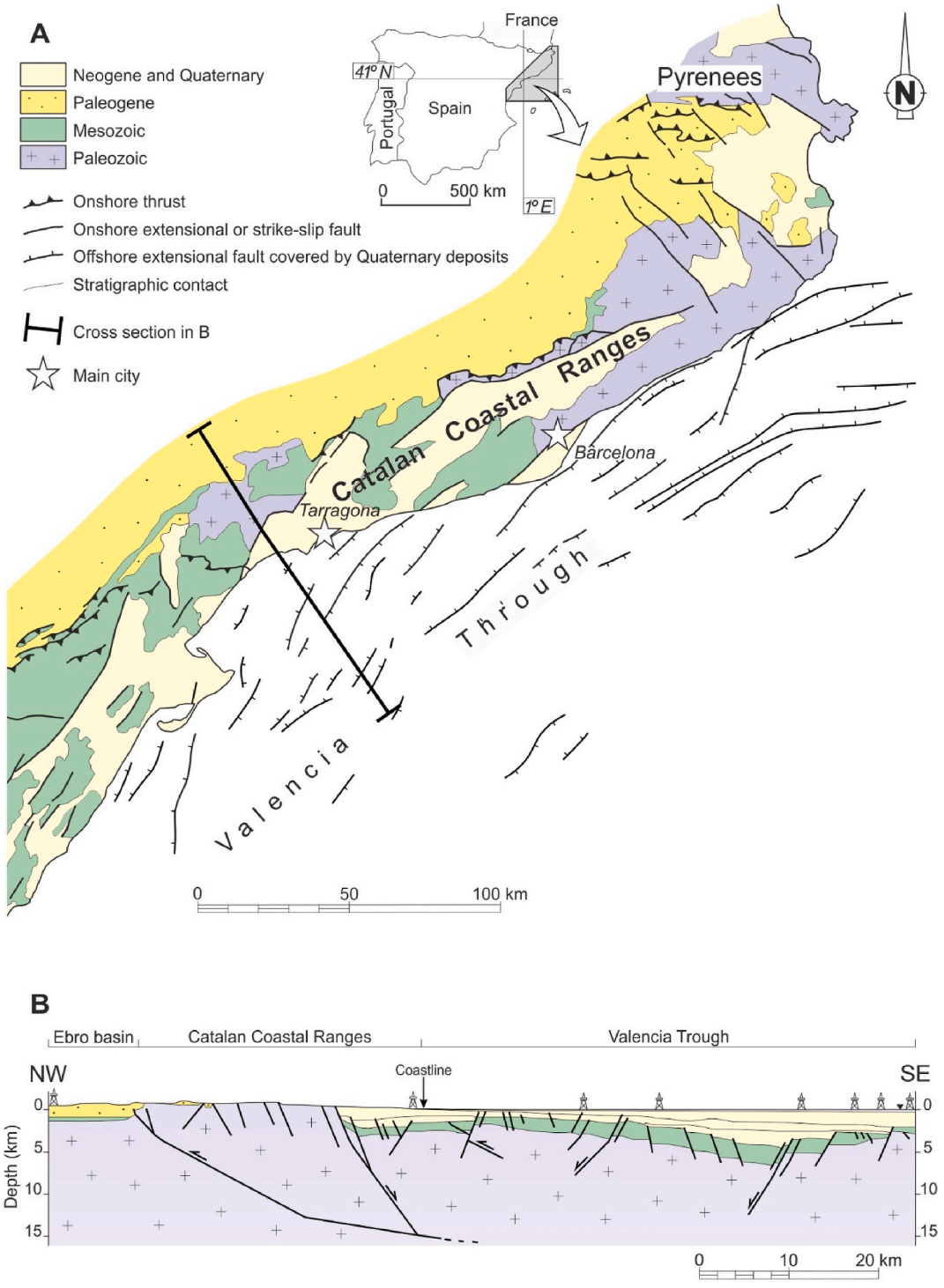

Fig. 2. A) Geological map of the northeastern part of the Iberian Peninsula and the northwestern margin of the Valencia Trough. After Roca (1994), Roca et al. (1999) and Barbara et al. (2019). B) Regional cross-section from the Ebro basin to the Valencia Trough. After Cabrera et al. (2004) and Bárbara et al. (2019).

The Castellón Group was defined as the sedimentary package limited by the underlying Alcanar Group and the overlying MES in the subsurface of the Valencia Trough (Clavell and Berastegui, 1991; Clavell, 1992; Martínez del Olmo, 2021). This lithostratigraphic unit can be subdivided in two formal units (Clavell, 1992), the Castellón Shales Formation and the Castellón Sandstones Formation, denoting the progradation of deltaic sediments in an overall shelfal setting. The Castellón Sandstones Formation overlies conformably on top of the Castellón Shales Formation, passing gradually from deep marine deposits to mainly wave-influenced shelfal deposits (Clavell and Berastegui, 1991; Clavell, 1992). The uppermost part of the Castellón Sandstones Formation is usually prominently truncated by the MES in the Valencia Trough, and regionally covered by the shale-rich Plio-Quaternary Ebro Shales Formation (Fig. 4).

3. Data and methods

The dataset used in this study comprises a wide range of well data including core, wireline logs (gamma ray, density, neutron and sonic) and well reports from five wells, the Amposta Marino C-2 well and Castellón B-7, B-9, B-1 and B-13 wells, and seismic data from three different cubes belonging to the Amposta, BG Ebro and Tortuga seismic surveys (Fig. 5), being the sedimentological description of the Amposta Marino C-2 well core the primary focus of this study.

The seismic dataset used in this study comprises three prestack time-migrated 3D seismic volumes covering an approximate area of 79 km^2 for the Amposta 3D cube, 2960 km^2 for BG Ebro 3D cube and 225 km^2 for the Tortuga 3D cube (Fig. 5). The analysis was done in time domain with a vertical resolution in the 20–30 m range depending on the seismic survey. The most common vertical exaggeration (V.E.) used for seismic interpretation was 5.

The workflow used in this study started with the sedimentological

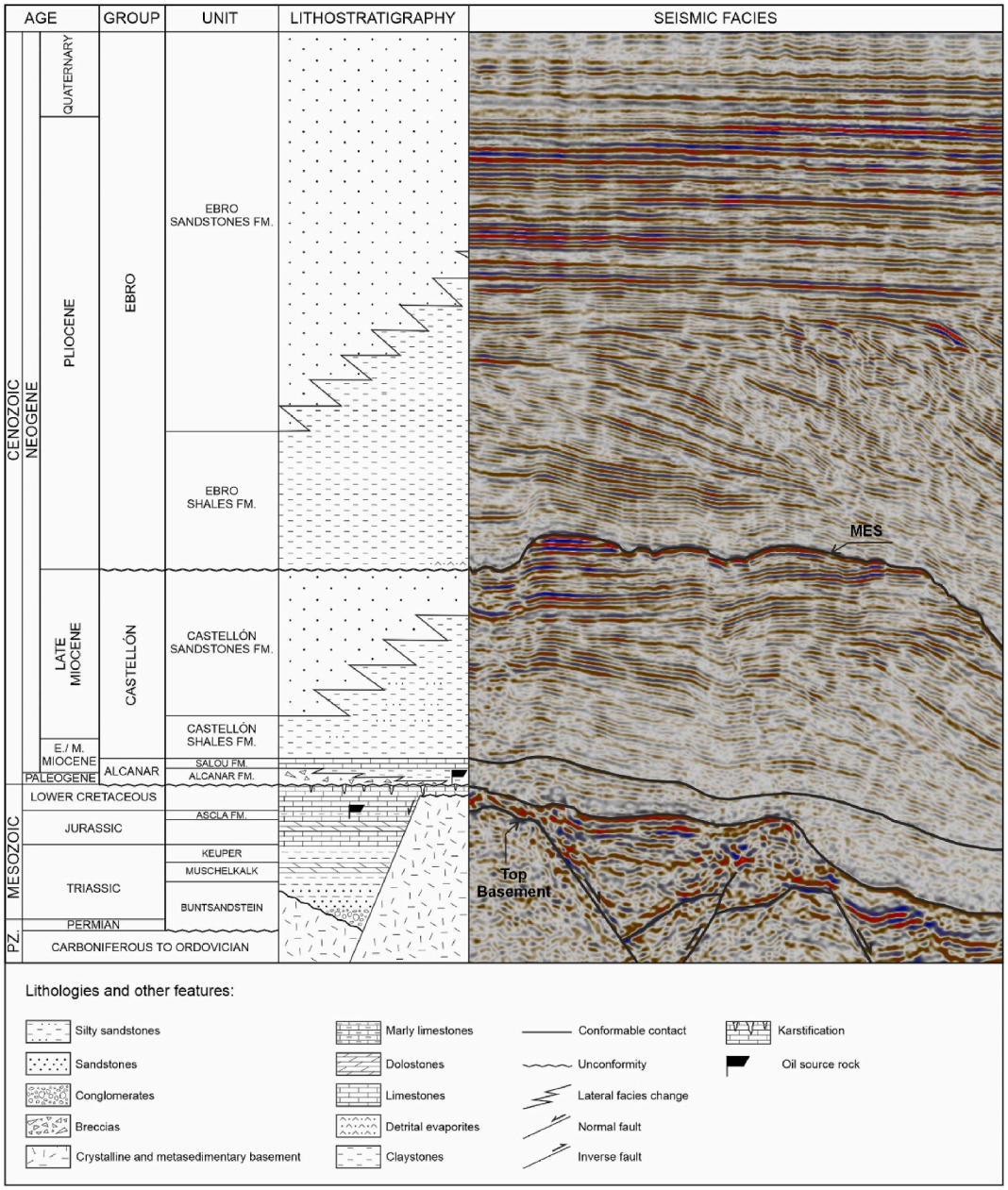

Fig. 3. Synthetic stratigraphic column with principal geological formations and ages (ages from Clavell, 1992). See also at the right-side of the figure a narrow representative seismic section showing the main seismic facies of each unit. E/M: Early to Middle; FM.: Formation; MES: Messinian Erosive Surface; PZ: Paleozoic.

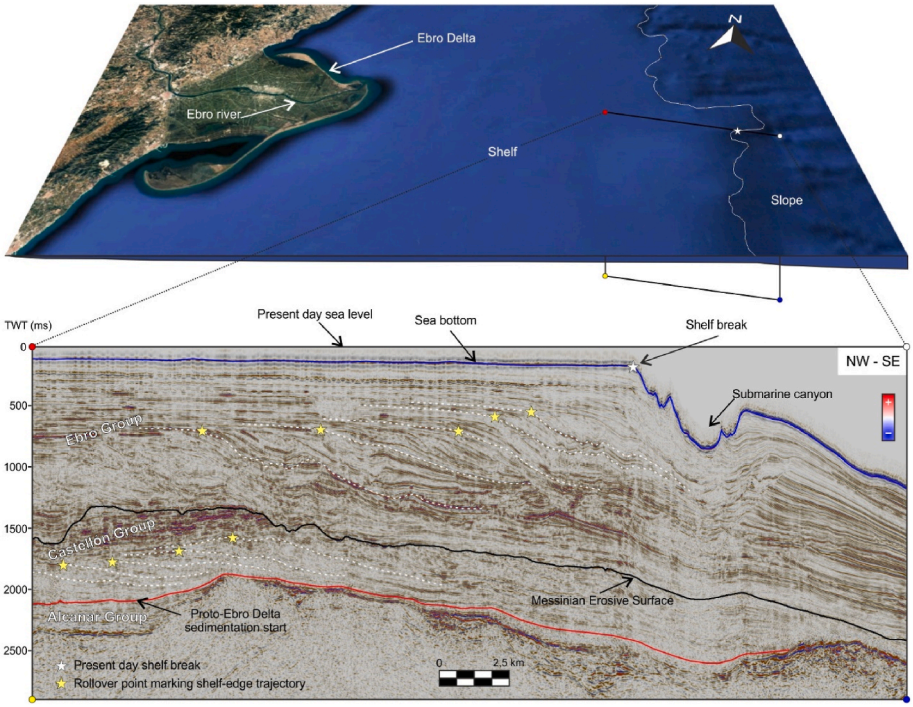

Fig. 4. Interpreted regional cross-section of the area with the seaward migration of the deltaic system along the time. Note the three main lithostratigraphic units above the Mesozoic: Alcanar, Castellón and Ebro Groups. The onset of the proto-Ebro delta sedimentation is interpreted in red, the MES is interpreted in black and the sea-bottom in blue (Vertical Exaggeration VE ~ 5). TWT stands for two-way travel time and is expressed in milliseconds (ms). Location of this seismic section is showed in Fig. 5. (For interpretation of the references to colour in this figure legend, the reader is referred to the Web version of this article.)

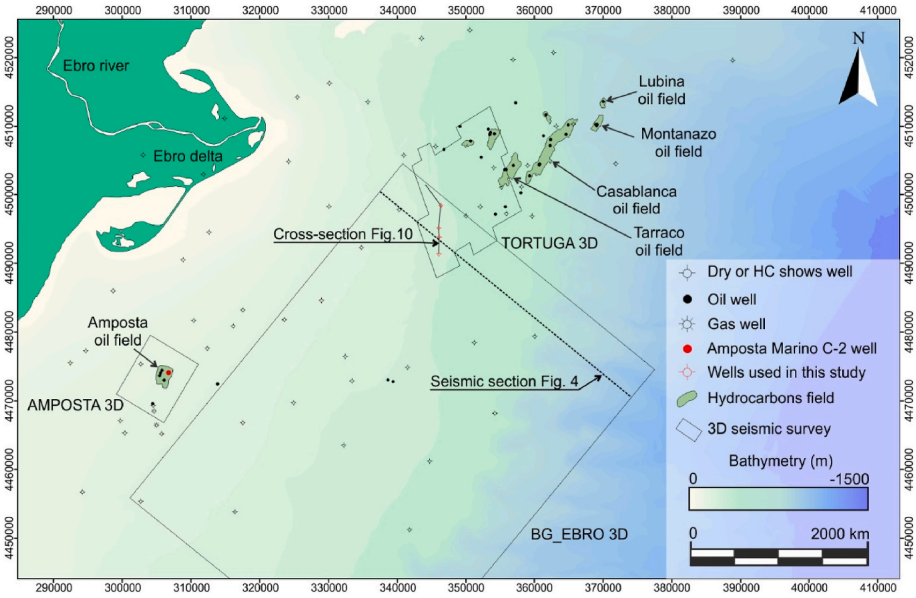

Fig. 5. Bathymetric map of the study area showing the four 3D seismic surveys used in this study and the historical wells in the zone. The main hydrocarbon fields are also represented. The Amposta Marino C-2 well analysed in this study is highlighted in red. Location of sections showed in Figs. 4 and 10 is also highlighted. (For interpretation of the references to colour in this figure legend, the reader is referred to the Web version of this article.)

description of the Amposta Marino C-2 well core, which includes 29 m of a continuous section of the upper part of the Castellón Sandstones Formation and a few centimetres of the lowermost interval of the Ebro Shales Formation. The sedimentological characterization of this core allowed to precisely interpret the facies associations present in this unit and to compare this hard core data with indirect rock measurements through the same logged section with conventional wireline logs.

In addition, a seismic stratigraphy analysis was done across the study area in order to interpret seismic facies with the aim of identifying and characterizing the main sedimentary packages with common aggradational, progradational or retrogradational stacking patterns in the study area and tie them to the patterns observed from the Amposta Marino C-2 well.

4. Results

4.1. Lithofacies

Eleven lithofacies were defined based upon their lithology, sedimentary structures and bioturbation type and intensity (Table 1) in the cored section of the Amposta Marino C-2 well (Fig. 6). Each lithofacies is described and interpreted as follows.

4.1.1. Burrowed calcarenites (Cb)

Lithofacies Cb is made of silty to very fine-grained calcareous sandstones with massive to slightly parallel and low-angle cross-lamination with scattered foraminifera, algae, bivalve and undetermined shell bioclasts. Subordinate lenticular bedding can also be observed. Bioturbation is moderate to intense with common *Planolites, Teichichnus* and *Thalassinoides* burrows (Fig. 7-A and B). The set thickness ranges from 10 to 30 cm.

The silty to very fine grain size composition of this lithofacies implies deposition in a relatively low-energy environment. The low-angle cross-lamination is interpreted as reflecting deposition from sand sheets or low relief sand bars in a subaqueous environment. Characteristic horizontal burrows point out an open marine outer to inner shelf environment dominated by deposit-feeding benthonic fauna.

4.1.2. Burrowed sandy heterolithics (HSb)

Lithofacies HSb is composed of intercalations of fine to very fined-grained sandstones with siltstones and silty claystones. Sandy layers are commonly present interlayered in the form of lenticular bedding with combined current and wave-ripple and flaser cross-lamination. Scattered bioclastic components of foraminifera, bivalve and undetermined shells are common. Bioturbation is moderate with common *Chondrites, Phycosiphon, Planolites, Teichichnus and Thalassinoides* burrows (Fig. 7-C). The set thickness ranges from 10 to 45 cm.

The silty to silty-clay fraction of this lithofacies implies deposition in a quite low-energy environment where smaller particles settled down in suspension. Sand-dominant intervals imply pulses of higher energy in a relatively protected or low energy environment.

4.1.3. Burrowed cross-bedded sandstones (Sxb)

Lithofacies Sxb is made of medium to fine-grained sandstones with common remnants of hummocky cross-stratification. Bioturbation is intense, especially in coarser-grained beds, obliterating most of the primary sedimentary structures. Characteristic observed horizontal traces include *Planolites, Teichichnus* and *Thalassinoides* (Fig. 7-D). The set thickness ranges from 10 to 30 cm with common inverse grading beds.

Coarser-grained sandstone layers appear to be linked to a higher bioturbation index. This is interpreted as an increase of organic matter in the sediment supplied by occasional hyperpycnal flows from a more proximal source. The presence of inverse graded beds with hummocky cross-stratification is interpreted as sedimentation of prograding bars and dunes in a subaqueous environment under the effect of a combined current flow, possibly in a middle to lower shoreface environment.

4.1.4. Cross-laminated calcarenites (Cx)

Lithofacies Cx is made of a slightly low-angle cross-laminated calcarenites with abundant algae bioclastic content (Fig. 7-E). Bioturbation was not observed. An individual bed was identified with a thickness of around 10 cm.

The calcareous composition of this interlayered bed in an overall sandy succession suggests change in accommodation and decrease in the siliciclastic sediment supply. Cross-lamination is interpreted as progradation of a dune or barform in a subaqueous environment.

4.1.5. Symmetrical ripple cross-laminated sandstones (Swr)

Lithofacies Swr is composed of medium to fine-grained, moderately

Table 1
Lithofacies scheme summarizing the main lithologies, bioturbation degree and type and main depositional process and/or interpretation. See Fig. 7 for detailed core pictures.

Code	Lithology	Lithofacies	Bioturbation	Interpretation
B	Breccia	Calcareous breccia	Not observed	Bioclastic lag in a marine setting
Cx	Calcarenites	Cross-laminated calcarenites	Not observed	Migration of dunes or barforms in a subaqueous environment
Cb		Burrowed calcarenites	Moderate to intense with common deposit-feeding ichnofauna	Sand sheets or low relief sand bars deposition in an open shallow marine environment
Sx	Sandstones	Cross-bedded sandstones	Not observed	Migration of dune and bar bedforms under conditions of net sedimentation in a moderate- to high-energy environment
Sr		Asymmetrical ripple cross-laminated sandstones	Rare to absent	Migration of current ripples under conditions of net sedimentation in a moderate- to high-energy environment
Swr		Symmetrical ripple cross-laminated sandstones	Rare to absent	Migration of wave ripples under conditions of net sedimentation in a moderate energy environment
Sv		Massive sandstones	Rare to absent	Dewatering and partial fluidization in a high sedimentation rate depositional setting
Sxb		Burrowed cross-bedded sandstones	Intense with common deposit-feeding ichnofauna	Migration of bars in an open shallow marine environment under the effect of a combined current flow, possibly in a middle to lower shoreface environment
Srb		Burrowed ripple cross-laminated sandstones	Low to moderate	Migration of current and wave ripples under conditions of net sedimentation. Sand was transported by combined unidirectional and oscillatory currents of low to moderate velocity
HSb	Heterolithics	Burrowed sandy heterolithics	Moderate with common deposit-feeding ichnofauna	Deposition in a low-energy marine environment where smaller particles settled down in suspension. Sand-dominant intervals imply pulses of higher energy in a relatively protected

(*continued on next page*)

Table 1 (*continued*)

Code	Lithology	Lithofacies	Bioturbation	Interpretation
				or low energy environment
HM		Muddy heterolithics	Not observed	Deposition of sandstone thin lenses by energetic pulses in an overall low-energy setting where mud settled out of suspension. Lack of bioturbation may represent anoxic conditions fairly distal marine setting

sorted sandstones with symmetrical ripple cross-lamination and locally intraclasts. Local flaser cross-bedding/lamination is observed (Fig. 7-F). Bioturbation is rare to absent. Cosets are typically showed with a thickness of 10–30 cm, whereas individual sets do not exceed 3 cm, typically associated with very thin silt to clay drapes.

The cross-lamination records the migration of symmetrical wave ripples under conditions of net sedimentation and implies that the sand was transported by an oscillatory current of low to moderate velocity above the storm wave base. The generalized lack of bioturbation indicates a moderate to relatively high energy environment.

4.1.6. Massive sandstones (Sv)

Lithofacies Sv are medium to fine-grained, poorly sorted, sandstones with poorly defined planar lamination and cross-bedding. Locally mud intraclasts, locally imbricated (Fig. 7-G), and soft-sediment deformation structures are present, the latter sometimes related to the presence of calcite cement bands. Bioturbation is rare to absent. The set thickness ranges from 5 to 20 cm.

The massive appearance of these lithofacies could be interpreted as the result of early postdepositional processes involving dewatering and partial fluidization, which may suggest a high sedimentation rate in the depositional system. Occasionally, the presence of calcite cement bands may obliterate previous primary sedimentary structures. The lack of detrital clays in these sandstones suggests deposition in a relatively high to moderate energy environment.

4.1.7. Burrowed ripple cross-laminated sandstones (Srb)

Lithofacies Srb is made of medium to very fine-grained sandstones, with combined symmetrical and asymmetrical ripple cross-lamination. Climbing ripples are locally observed. Bioturbation index is low to moderate. Most traces correspond to undetermined horizontal burrows (Fig. 7-H–J) sometimes linked to soft-sediment deformation laminae. Sets/cosets are typically observed with a thickness of 5–15 cm, typically associated with very thin silt to clay drapes.

The cross-lamination records the migration of current and wave ripples under conditions of net sedimentation and implies that the sand was transported by combined unidirectional and oscillatory currents of low to moderate velocity. The presence of bioturbation possibly reveals deposition in a shallow to marginal marine environment.

4.1.8. Calcareous breccia (B)

Lithofacies B is composed of a very coarse-grained calcareous clast-supported breccia that mainly contains bivalve, coral, foraminifera and undetermined shell bioclasts. A prominent erosive base bound this lithofacies and occasional large centimetric mud intraclasts are present (Fig. 7-K and N). High calcite cementation is common in between bioclastic components.

The erosive base limiting this shell beds, the large amount of bioclastic content and presence of mud clasts are interpreted in terms of a bioclastic lag deposited in an open marine environment.

4.1.9. Cross-bedded sandstones (Sx)

Lithofacies Sx is composed of medium-, locally coarse-grained, moderately to poorly sorted sandstones with high-angle foresets (>15°). Locally, mud drapes and mudstone clasts line set bases and foresets (Fig. 7-L). Evidence of bioturbation in this lithofacies was not found. The sandstones form 30 to 60 cm-thick sets, commonly bounded by a basal erosive surface and present normal grading beds. Unidirectional and/or bidirectional ripple cross-lamination is locally observed especially towards the upper part of the sets.

Cross-bedding is interpreted as a response to the migration of dune and bar bedforms under conditions of net sedimentation. Local mud drapes at the top of normal graded layers reflect alternating periods of waxing and waning of possibly hyperpycnal flows sedimentation. The generalized lack of detrital clays and bioturbation suggests moderate-to high-energy conditions, under which fines were carried off in suspension.

4.1.10. Asymmetrical ripple cross-laminated sandstones (Sr)

Lithofacies Sr is made of medium to fine-grained sandstones, moderate to poorly sorted sandstones with asymmetrical or unidirectional ripple cross-lamination and locally intraclasts (Fig. 7-M). Bioturbation is rare to absent. Cosets typically present a thickness of 10–20 cm, whereas individual sets do not exceed 5 cm, typically associated with very thin silt to clay drapes.

Cross-lamination records the migration of current ripples under conditions of net sedimentation and reveals that sand was transported by a unidirectional current at low-to moderate-velocity. The generalized lack of bioturbation indicates a non-marine and/or moderate to high energy environment.

4.1.11. Muddy heterolithics (HM)

Lithofacies HM are calcareous claystones (marls) interbedded with siltstone and very fine-grained sandstone. This facies shows planar lamination and rare lenticular bedding with rippled sand lenses. Bioturbation was not observed. This lithofacies is restricted to the uppermost part of the cored section and belongs to the onset of the Ebro Shales Formation.

The sandstone thin lenses represent energetic pulses in an overall low-energy setting where mud settled out of suspension. During the higher energy pulses, sand was moved by turbulent flows downstream. The lack of bioturbation indicates anoxic conditions in a fairly distal marine setting.

4.2. Facies associations of the Castellón Sandstones Formation

Interpretation from previous lithofacies description allows to propose a scheme of six facies associations designated as follows, from proximal to distal (Fig. 8).

4.2.1. Fluvial channel (FC)

Facies association FC mainly consists of lithofacies Sx and Sr (Fig. 8). The thickness of individual packages of this facies association ranges from 25 to 90 cm and shows an aggrading to fining-upward stacking pattern. The basal contact of this package is erosive and corresponds to the MES. Evidence of bioturbation was not found. The gamma ray profile of this facies association is showed as a bell shape profile, characterised by values ranging from 50 to 81 API. This facies association is interpreted as possibly non-marine channel deposits based on the lack of bioturbation and marine fossils and characteristic waning signal of channel infill from high energy sand bars migration (lithofacies Sx) to lower energy current ripples (lithofacies Sr) migration on top. The lack of associated floodplain deposits at this location opens the interpretation to a wide set of depositional environments. However, the bad sorting of these sandstones encourages us to link these deposits within a quite

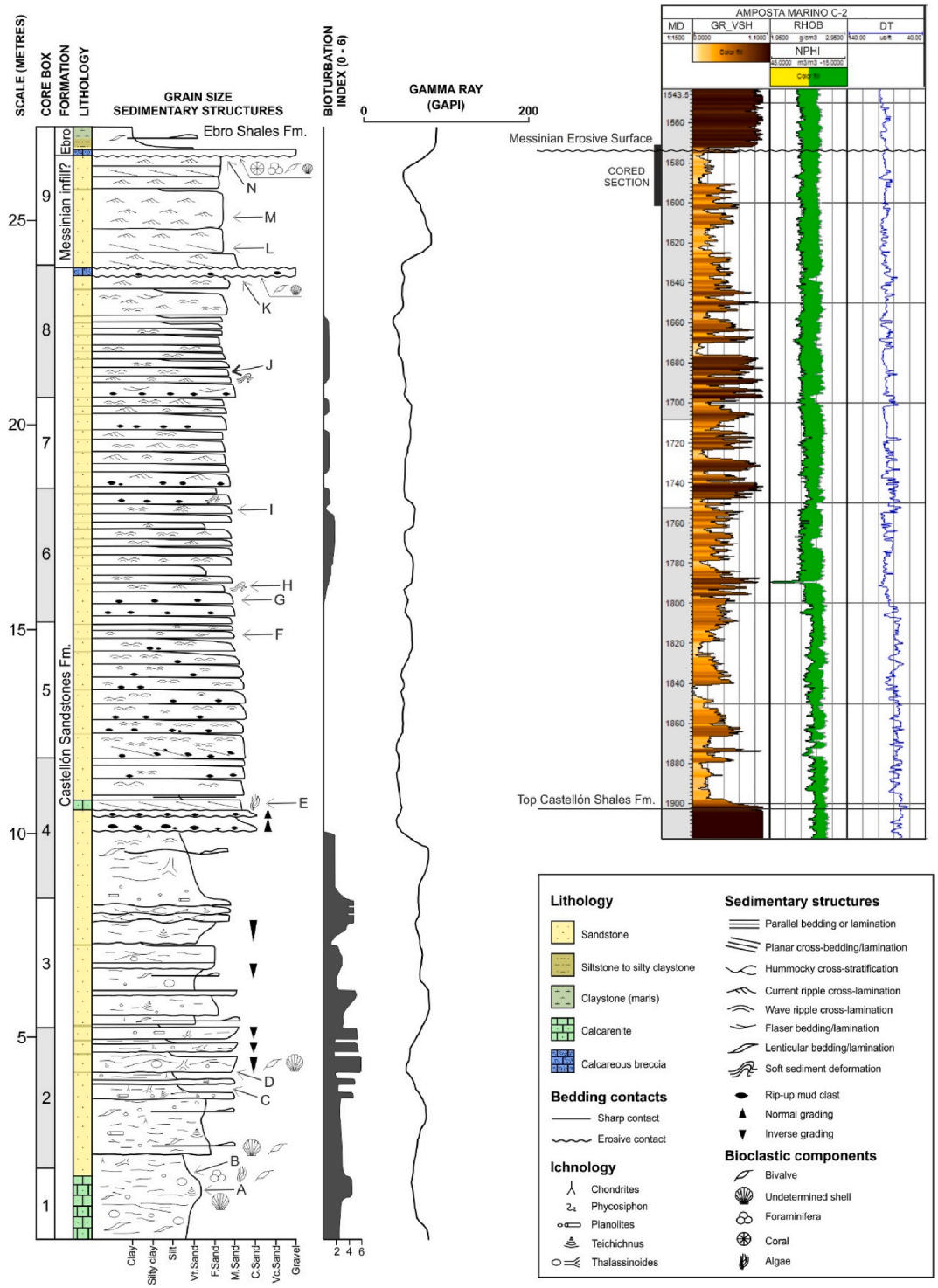

Fig. 6. Composite stratigraphic column of the cored section of well Amposta Marino C-2 (AMC-2) showing the main sedimentological features, bioturbation index and gamma ray profile. The A – N capital letters on the stratigraphic column correspond to detailed sedimentary structures and rock fabrics of lithofacies observed in the core, which are displayed in Fig. 7. See also a well composite from AMC-2 at the upper right side of the figure displaying, from left to right, the normalized shale volume from gamma ray (GR_VSH), density-neutron and sonic (DT) wireline logs and the location of the cored section. The depths of the Messinian Erosive Surface and the top of the Castellón Shales Formation are also displayed. See location of the well in Fig. 5.

proximal setting, at least an upper delta plain or even a more proximal depositional environment. The thickness of this package is under the vertical resolution of the seismic surveys, although some studies have proved the presence of a fluvial drainage system related with the MES in the area of study (Cameselle and Urgeles, 2015; Urgeles et al., 2011). Porosity values measured on plugs under conventional core analysis range from 13 to 24 % (Fig. 8).

4.2.2. *Delta front proximal mouth bar (DFPMB)*

Facies association DFPMB is composed of lithofacies Sx, Swr, Sr, Sv, Srb, HSb and Cx (Fig. 8). It is organized in 30–90 cm-thick individual bed sets, typically bounded by an erosive base with common mud clasts.

The stacking pattern is aggradational to progradational. Bioturbation is typically low to absent, probably denoting the moderate to high energy conditions of the system. Ichnotaxa identified include *Phycosiphon*, *Planolites*, *Teichichnus* and *Thalassinoides* traces and are almost exclusively found into the HSb lithofacies. The gamma ray log shows for this facies association a funnel shape profile, with values ranging from 61 to 43 API in an overall clean sand package. This facies association is interpreted as delta front proximal mouth bar deposits based on the aggradational to progradational stacking pattern of these deposits and the combination of both unidirectional and oscillatory current sedimentary structures, which denotes a dominant progradation direction of sand-prone deposits and reworking by wave action close to the shoreline. Lithofacies HSb and Cx may indicate a relative distal location of these proximal mouth bar deposits and/or a fringe/interbar position with relatively lower energy conditions in a shallow marine environment. Measured porosity values from conventional core analysis (CCA) range from 17 to 23 % (Fig. 8).

4.2.3. Delta front distal mouth bar (DFDMB)

Facies association DFDMB consists of Sxb, Srb and HSb (Fig. 8). It is typically arranged in 20–80 cm-thick packages with a common progradational stacking pattern. Bioturbation is moderate to intense, especially in the more heterolithic sections. Ichnotaxa identified include *Phycosiphon*, *Planolites*, *Teichichnus* and *Thalassinoides* burrows. The

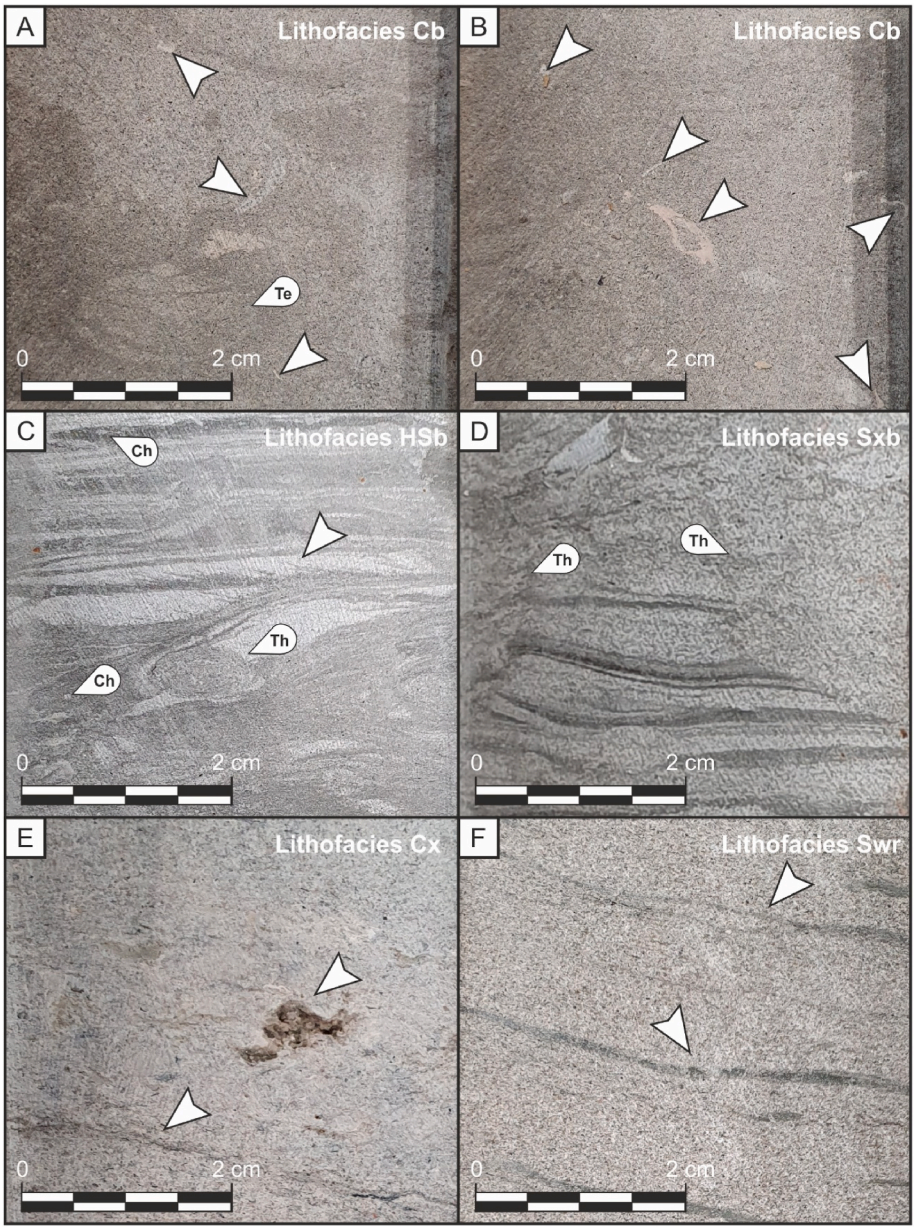

Fig. 7. Detailed core pictures with the most characteristic lithofacies features. A) Burrowed calcarenite with common bioclasts and *Teichichnus* burrows; B) Burrowed calcarenite with abundant bioclasts; C) Burrowed sandy heterolithics with *Chondrites* and *Thalassinoides* ichnotaxa and interlayered mud-draped ripple cross-lamination; D) Burrowed cross-bedded sandstones with *Thalassinoides* burrows; E) Cross-laminated calcarenites with vuggy porosity associated to algae bioclastic content. See also the silty lineation draping the lamination; F) Flaser cross-lamination and silt to mud drape on a wave ripple cross-lamination; G) Imbricated mud clasts in massive sandstones; H) Soft-sediment deformation triggered by biological activity on burrowed ripple cross-laminated sandstones; I) Silt to mud-draped climbing ripples in burrowed ripple cross-laminated sandstones; J) Indeterminate trace on burrowed ripple cross-laminated sandstones.
Fig. 7. – **(Continued)** K) Calcareous breccia with large centimetric bioclasts and local mud intraclasts; L) High-angle cross-bedded sandstones; M) asymmetrical current ripple-cross laminated sandstones. Notice the direction of migration of the ripples toward the left; N) Calcareous breccia with characteristic coral and shell fragment bioclasts. Ch: *Chondrites*; Te: *Teichichnus*; Th: *Thalassinoides*.

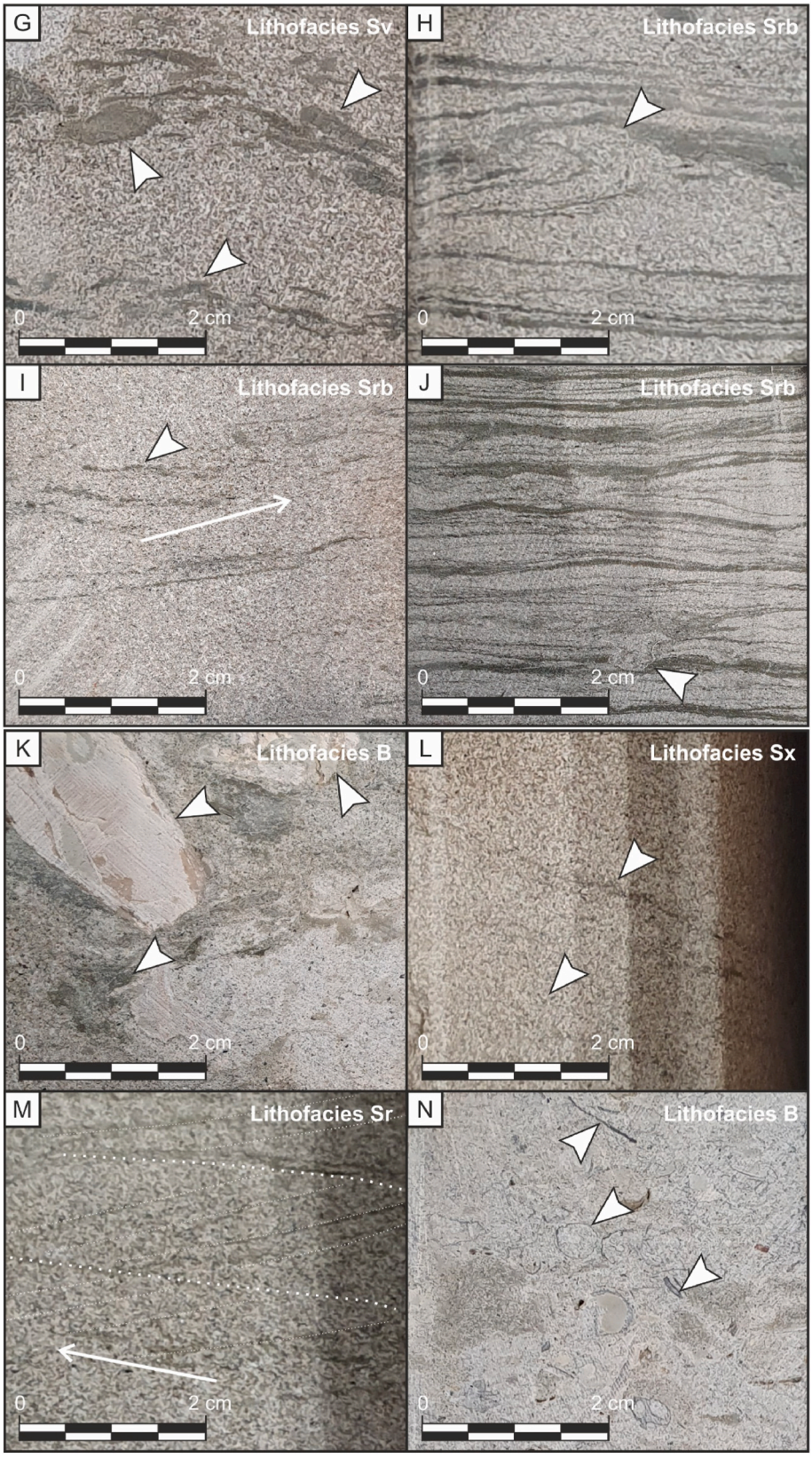

Fig. 7. (*continued*).

gamma ray log is presented with a funnel shape ranging values from 75 to 50 API. This facies association is interpreted as delta front distal mouth bar deposits based on the progradational stacking pattern of sandy to heterolithic deposits with characteristic marine bioturbation. Cross-bedding in sandstones is interpreted as hummocky cross-stratification, denoting deposition and/or reworking by wave action during storm events in a middle to lower shoreface setting. Measured porosity values from CCA range from 16 to 20 % (Fig. 8).

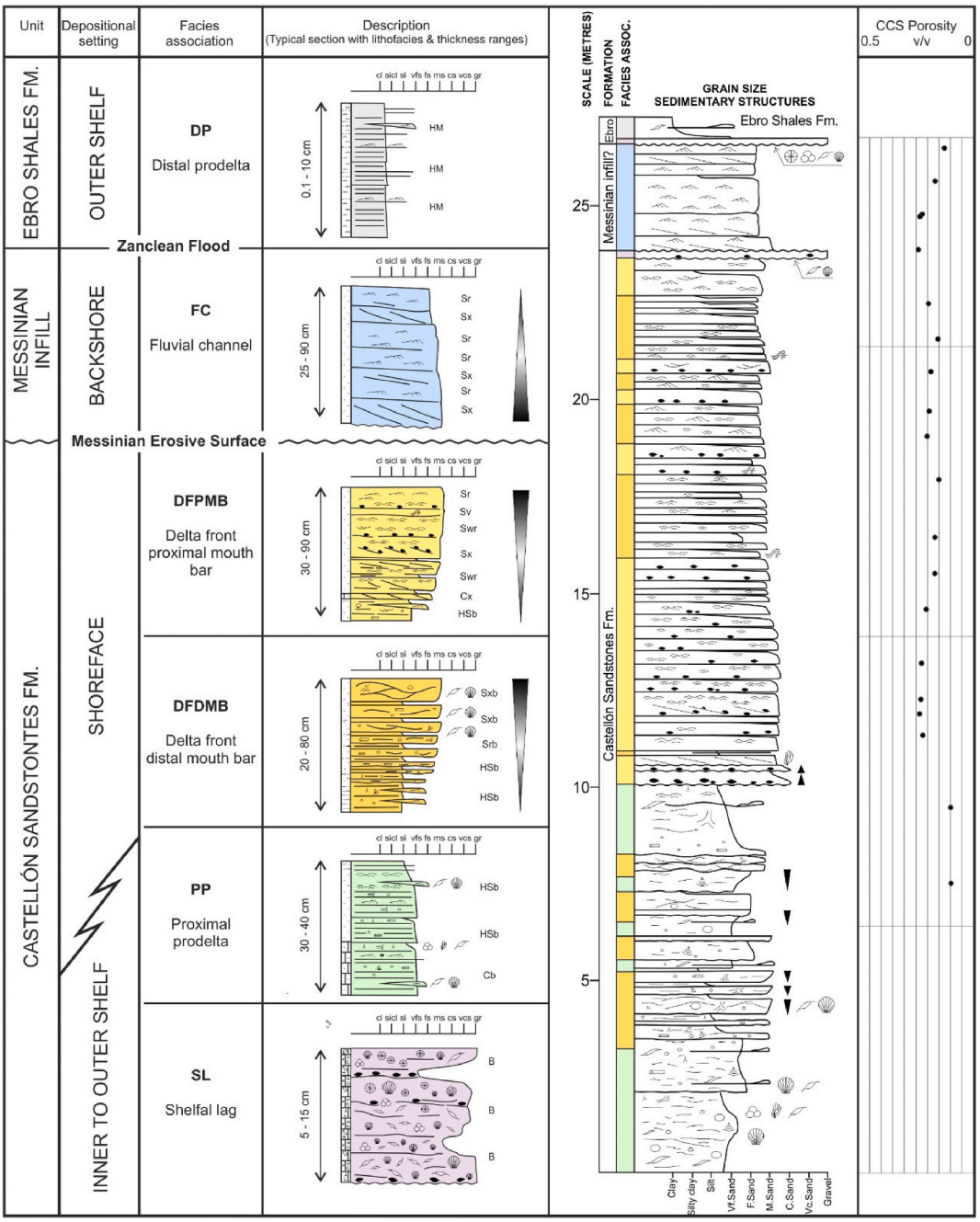

Fig. 8. Schematic summary of facies associations (FA) with a synthetic stratigraphic column that includes the main lithofacies, their average thickness, bioturbation, stacking patterns and the bioclastic components, based on the cored section described from the Amposta Marino C-2 well (AMC-2). The main units and depositional settings are also represented at the left-hand side of the figure. Considering the progradational trend of the Castellón Sandstones Formation, the facies associations are roughly represented from distal to proximal from the bottom to the top of the figure with the main discontinuities found in the cored section of AMC-2 represented. See also at the right-hand side of the figure, the cored section of AMC-2 with the FA interpreted and porosity data from conventional core analysis (CCA).

4.2.4. *Proximal prodelta (PP)*

Facies association PP mainly consists of lithofacies Cb and HSb (Fig. 8). It is organized in 30–40 cm-thick conformable packages with gradational contacts. The stacking pattern is typically aggradational to slightly progradational. Bioturbation is moderate to intense with common marine ichnotaxa such as *Chondrites, Phycosiphon, Planolites, Teichichnus and Thalassinoides*. The gamma ray profile of this facies association is commonly seen as a funnel shape with values ranging from 68 to 90 API. This facies association is interpreted as proximal prodelta mainly based on the heterolithic-prone fabric, marine ichnotaxa and on the presence of combined current and wave-ripple cross-lamination, which indicates that these deposits where sedimented above the storm wave base of an open marine shelfal environment. Gradation from a calcarenitic to a siliciclastic fabric may reveal changes in sediment supply triggered by allocyclic controls and/or autocyclic lateral avulsion of mouth bar deposits in a more proximal domain, allowing to carbonate shelfs to develop in the fringe zone or interbar position of dominant siliciclastic delta front deposits. Measured porosity values from CCA is around 10 % (Fig. 8).

4.2.5. *Distal prodelta (DP)*

Facies association DP is formed of lithofacies HM in the cored section (Fig. 8). It is organized in mm-to cm-thick silt to calcareous claystone laminae interbedded with rare very fine-grained sandstone lenses with

ripples. Bioturbation was not found in this facies association. The gamma ray profile of this facies association is serrated with very high values, generally above 90 API, and most commonly above 110 API values. It is only found at the uppermost part of the cored section of Amposta Marino C-2 well (Fig. 6). This facies association belongs to the onset of the Ebro Shales Formation. However, its presence is also expected in lower sections of the Castellón Sandstones Formation and in the underlying Castellón Shales Formation due to the progradational pattern of this succession. It is interpreted as distal prodelta deposits in a fairly distal marine setting, based on the fine-grained fabric of these deposits, the lack of bioturbation which may indicate relatively low oxygen level in a deepwater setting and the presence of occasional interbedded sand lenses sedimented by hyperpycnal flows in an open marine distal environment. There is not measured values of porosity for this facies association.

4.2.6. Shelfal lag (SL)

Facies association SL consists of lithofacies B (Fig. 8). It can be found organized in 5–15 cm thick packages grouped in two distinct layers across all the studied cored section. The base is erosive with occasional mud clasts on top and is made of very coarse-grained carbonate bioclastic grains with a dispersed internal lamination, forming a calcareous breccia. The limited thickness of these packages are under the resolution of the gamma ray and make them not possible to identify with this tool.

These shell beds are interpreted to have been deposited under a low net sedimentation rate in a starved basin margin or in an open shelf associated with a transgression (Cattaneo and Steel, 2003). There are no porosity measurements for this facies association.

4.3. Seismic stratigraphic analysis

After screening the 3D seismic surveys through the whole study area, at least three different seismic facies have been identified within the Castellón Sandstones Formation (Fig. 9). They are, from bottom to top, as follows.

4.3.1. Prodelta seismic facies

The onset of the Castellón Sandstones Formation is marked by the entry of coarser sediment into the basin under an overall framework of progradation of the Castellón Group deltaic complex. The background is characterized by fine-grained sediment identified from the seismic dataset by low amplitude, transparent and semicontinuous reflectors with a progradational to aggradational stacking pattern. The topsets and foresets of the identified clinothems start to show higher amplitude reflectors, probably reflecting the presence of coaser-grained sediment, interpreted in terms of shelfal lobes rimming the shelf margin (Fig. 9). Occasional higher amplitude, semicontinuous reflectors with a characteristic channel-levee shape are also seen in the foreset to bottomset

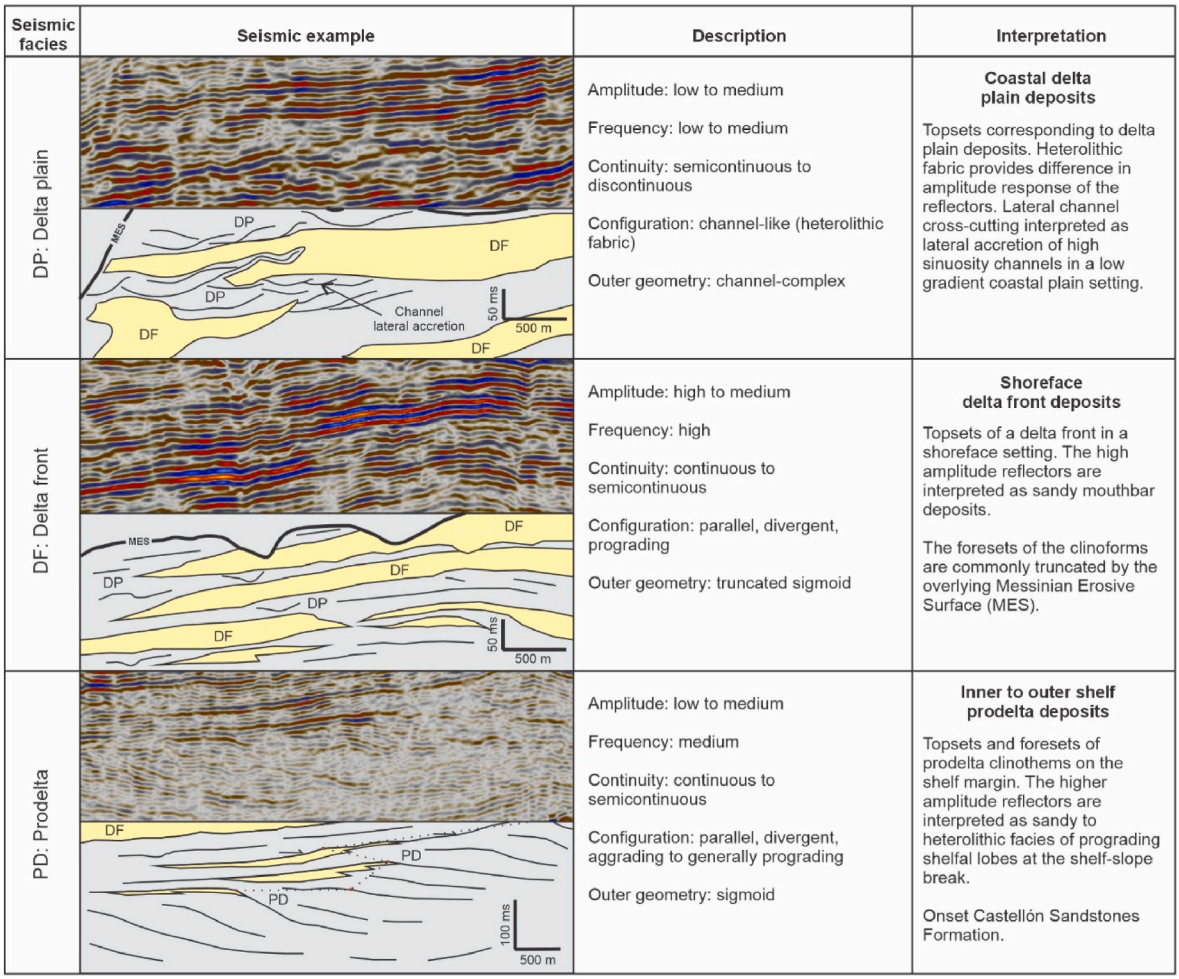

Fig. 9. Summary of the main seismic facies identified for the Castellón Sandstones Formation in the study area with their interpretation below. From base to top: PD: Prodelta seismic facies with the shelf-break evolution represented by a dashed line; DF: Delta front seismic facies; DP: Delta plain seismic facies. Yellow colour background is linked to sand-prone deposits and grey colour background is linked to shale-to heterolithic-prone deposits. Examples extracted from BG_Ebro 3D seismic survey. MES: Messinian Erosive Surface. (For interpretation of the references to colour in this figure legend, the reader is referred to the Web version of this article.)

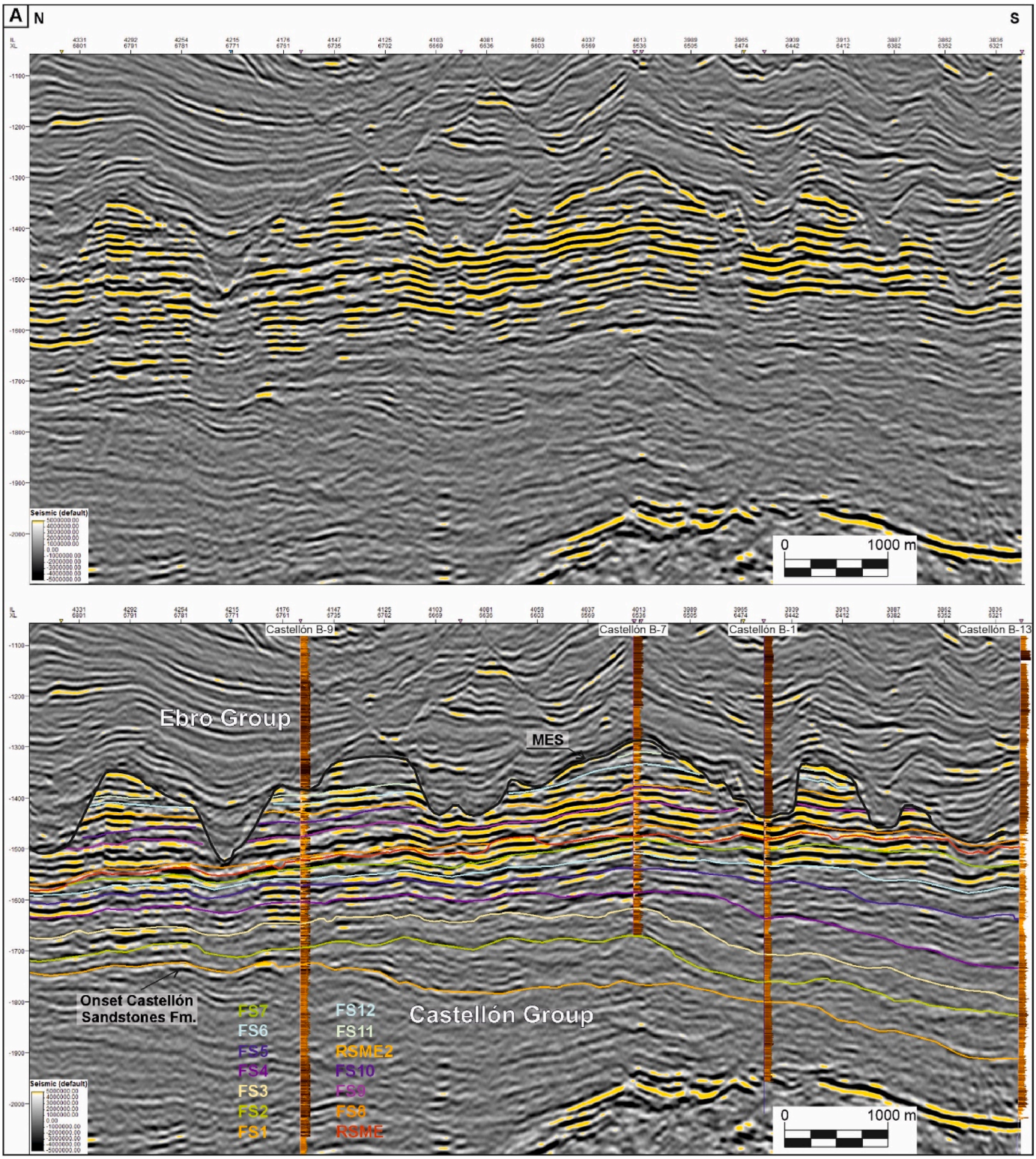

Fig. 10. A) Uninterpreted (above) and interpreted (below) seismic cross-section, correlating from left to right, Castellón B-9, B-7, B-1 and B-13 wells. Gamma Ray profile is displayed in each well. The legend for the horizons is displayed in the lower part of the interpreted section. See the location of the seismic cross-section in Fig. 5.

Fig. 10. **(continued) –** B) Detail of a transition from prodelta to proximal delta front facies associations represented in seismic and wireline log data. C) Detail of characteristic delta plain deposits observed both, in seismic and wireline log data. Detail images showed in B) and C) come from Castellón B-7 well. D) North-south oriented correlation panel among the Castellón wells. Facies associations based on wireline log response are interpreted in each well. Main interpreted horizons, including flooding (FS1 to FS12) and erosive surfaces (RSME and RSME2) are also showed. See also the diachronous position of the onset of the Castellón Sandstones Formation, highlighted with a red star in each well. FS: Flooding Surface; MES: Messinian Erosive Surface; RSME: Regressive Surface of Marine Erosion. (For interpretation of the references to colour in this figure legend, the reader is referred to the Web version of this article.)

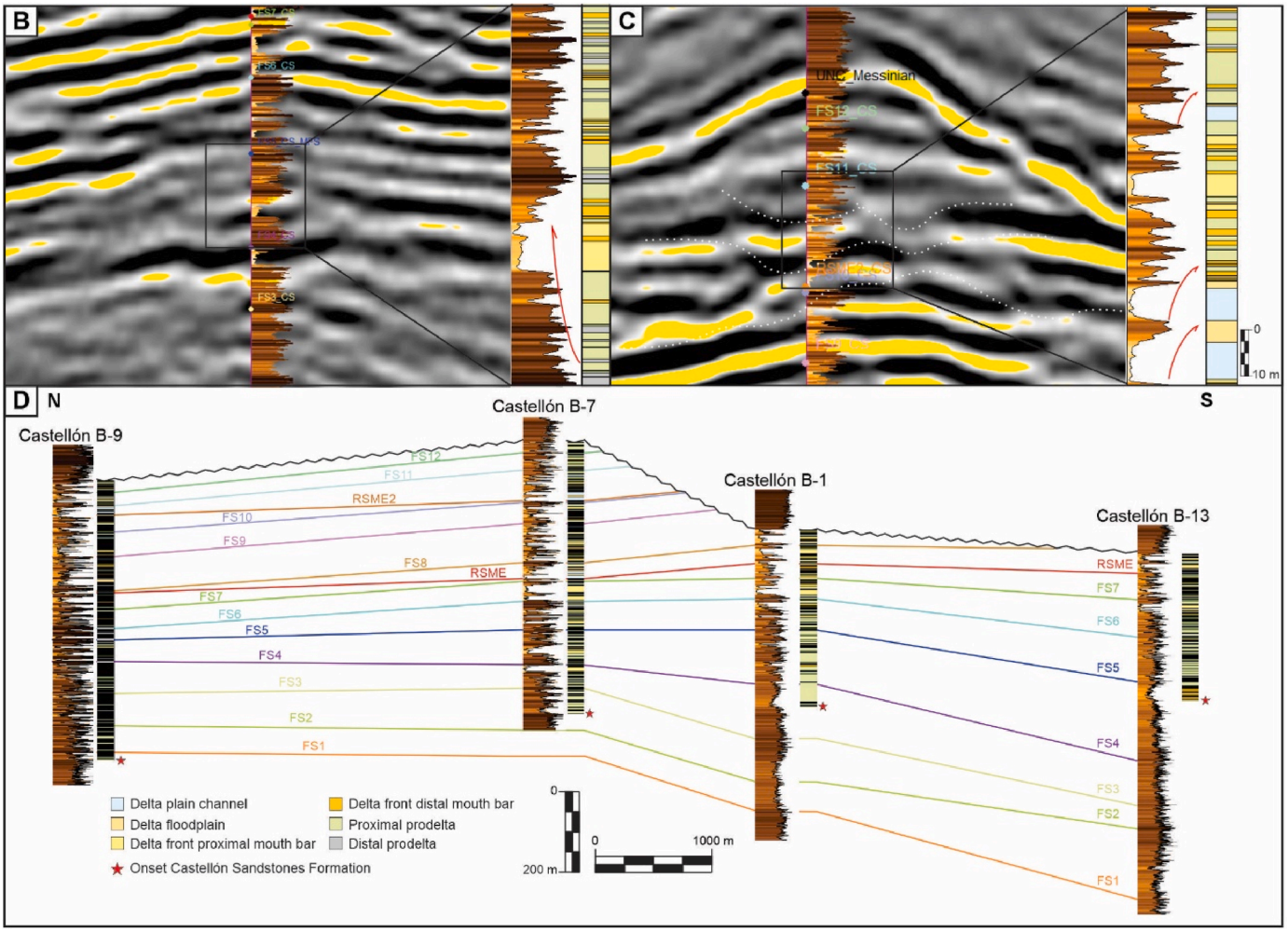

Fig. 10. (*continued*).

position. These deposits might be associated with thin sandy packages that overpassed the shelf-break and are interpreted as turbiditic deposits sedimented in a deep marine slope environment.

4.3.2. Delta front seismic facies

Continuing with the regressive trend observed in the seismic profiles, the prodelta seismic facies evolve vertically to high-amplitude, continuous to semicontinuous and parallel-organized reflectors with a prograding to aggrading stacking pattern. They are interpreted as delta front deposits (Fig. 9). The high amplitudes of these reflectors is probably linked to the amalgamation of sand-rich mouth bars, as also interpreted from the cored section of Amposta Marino C-2 well. The apparent lateral connectivity of these deposits is fair to good in many occasions. In contrast, the vertical connectivity of these bodies remains uncertain, as the vertical resolution of the seismic dataset precludes the identification of shale-to heterolithic-prone deposits interlayered between these sandy packages. In other cases, low-to medium-amplitude, transparent to discontinuous reflectors are clearly bounding some of these deposits and are interpreted as shale-to heterolithic-prone deposits of the following seismic facies.

4.3.3. Delta plain seismic facies

Culminating the preserved section of the Castellón Sandstones Formation in the area of study, low-to medium-amplitude, semicontinuous to discontinuous reflectors can be identified, also revealing characteristic channel-shape geometries. These are interpreted as possibly delta plain deposits with the presence of fluvial channels with relatively high sinuosity, as seen by cross-cutting relationships. They are interpreted to result from lateral migration of channels in a low gradient coastal setting (Fig. 9). The frequent transparent aspect of this facies may reveal a shale-to heterolithic-prone fabric, characteristic of a delta plain setting, where distributary channels are interlayered with fine grained floodplain deposits. This seismic facies is typically truncated by the MES and capped by low-amplitude, transparent and semicontinuous reflectors associated with the shale-prone deposits of the Ebro Shales Formation. In some cases, higher amplitude, continuous to semicontinuous reflectors with channel-levee shape, are present in contact with the MES. These are interpreted in terms of deep marine turbiditic deposits associated with bottomset slope deposits. Furthermore, some high-amplitude reflectors are occasionally seen infilling topographic lows of the MES paleorelief. These could also be associated with lowstand fluvial deposits related to the Messinian infill.

4.4. Sedimentary architecture of the Castellón Sandstones Formation

The Castellón Sandstones Formation has a maximum thickness around 850 m and extends for hundreds of kilometres across the study area and further to the north-northwest, at least up to the present-day coastline and to the south-southeast, before dramatically reducing its thickness and getting condensed into deeper waters of the Valencia Trough.

The erosion produced by the MES constitutes a challenge for correlation between wells and inference of potential reservoir sedimentary architecture into delta front and delta plain facies belts. In order to get

insight on this purpose, a first correlation between Castellón B-6, B-7, B-1 and B-13 wells has been carried out (Fig. 10).

A series of 14 surfaces have been linked along this cross-section allowing the lateral correlation of major sedimentary packages among these wells. Support from seismic data has become key to correlate clinoform surfaces across a selected zone in the study area. Twelve out of these fourteen horizons are interpreted as flooding surfaces (FS1 to FS12), showed in well log data as peaks in the gamma ray profile, typically constituted by very high shale content. The other two horizons are erosive in character (RSME and RSME2) and can be identified in gamma ray logs, constituting the base of clean sandy packages, as well as in seismic as erosional unconformities extending widely across the study area. The sequence stratigraphic meaning of the interpreted surfaces is discussed later in the discussion section.

The facies associations found in Castellón B wells area shows a dominance in delta front and prodelta deposits at the basal part of the Castellón Sandstones Formation (Fig. 10-A), vertically evolving to delta front and delta plain facies deposits. This trend can be observed both, in well log data as coarsening-upwards sequences grading from shaly prodelta deposits at the base to cleaner sandy delta front deposits to the top (Fig. 10-B), and in seismic data as prograding continuous to semi-continuous, transparent low amplitude reflectors, characteristic of prodelta deposits, grading upwards to continuous, higher amplitude and frequency reflectors to the top, interpreted as delta front deposits.

In contrast to Amposta Marino C-2 well area (Fig. 5), Castellón B wells clearly shows the presence of delta plain deposits. In well log data, they are identified as 2–10 m thick sandy packages with a fining-upwards profile in gamma ray, probably showing the waning effect in the deposition of fluvial channels in a delta plain. This fact is supported by moderate to high amplitude channelized bodies in seismic, surrounded by more transparent and discontinuous background in the topset of clinothems, occasionally with a lateral migration pattern (Fig. 10-C). These are interpreted as lateral accretion packages corresponding to high sinuosity channels migrating in a heterolithic delta floodplain.

The correlation among these wells shows an overall sedimentary trend from dominantly proximal delta plain and delta front proximal mouth bar deposits in the north-northwest area to distal mouth bar and proximal prodelta deposits towards the south-southeast (Fig. 10-D). This trend correspond with the progradation of the proto-Ebro delta during the Late Miocene in the Valencia Trough. This fact is also highlighted by the diachronous onset of the Castellón Sandstones Formation in the area, as interpreted in the correlation panel among the Castellón wells (Fig. 10-D).

5. Discussion

The results indicate that the Castellón Sandstones Formation is made of deltaic deposits that were sedimented in a transitional marginal to shallow marine depositional setting. Lithofacies and facies associations characterized from the cored section of the Amposta Marino C-2 well show a characteristic fluvial dominance over subordinate wave action on sedimentary processes controlling the sedimentation of this succession. Hummocky cross-stratification on distal delta front deposits points out towards a sediment wave modelling on a lower to middle shoreface setting, as well as the presence of oscillatory wave ripples on delta front and prodelta deposits. However, the generalized presence of unidirectional current sedimentary structures, such as asymmetrical ripples and planar cross-bedding, together with a moderate to bad sorting of sandstones in proximal delta front mouth bar deposits, suggest a river-dominated delta modelled by waves as the most likely sedimentary model for the Castellón Sandstones Formation (Fig. 11).

The seismic facies (Figs. 9 and 10) observed further to the east into the Tortuga area proved that this delta was also represented by a set of facies associations not represented, or even present, in the Amposta area, such as delta plain deposits. This fact exposes the importance of identifying potential shale-rich intervals, as delta plain deposits, due to the role of shale layers and heterolithics in the distribution and main fairways for the CO_2 plumes in the subsurface after its injection and storage (Williams and Chadwick, 2021).

Most of the facies associations containing sand-prone packages present good petrophysical properties (Fig. 8), being the fluvial channels (with an average porosity of 18.5 %), the delta front proximal mouth bar (with an average porosity of 20 %) and the delta front distal mouth bar (with an average porosity of 18 %) deposits the facies associations with better reservoir potential. On the other hand, Distal Prodelta facies associations present a predominant muddy fabric, which apparently present a high potential as a vertical seal (Martín-Monge et al., 2024), although further work will be needed to quantify the sealing capacity of these facies under in situ storage conditions. The high cementation present in shelfal lag levels may also act as local baffles for fluid flow. Occasional fluvial channel deposits mainly infilling MES paleorelief

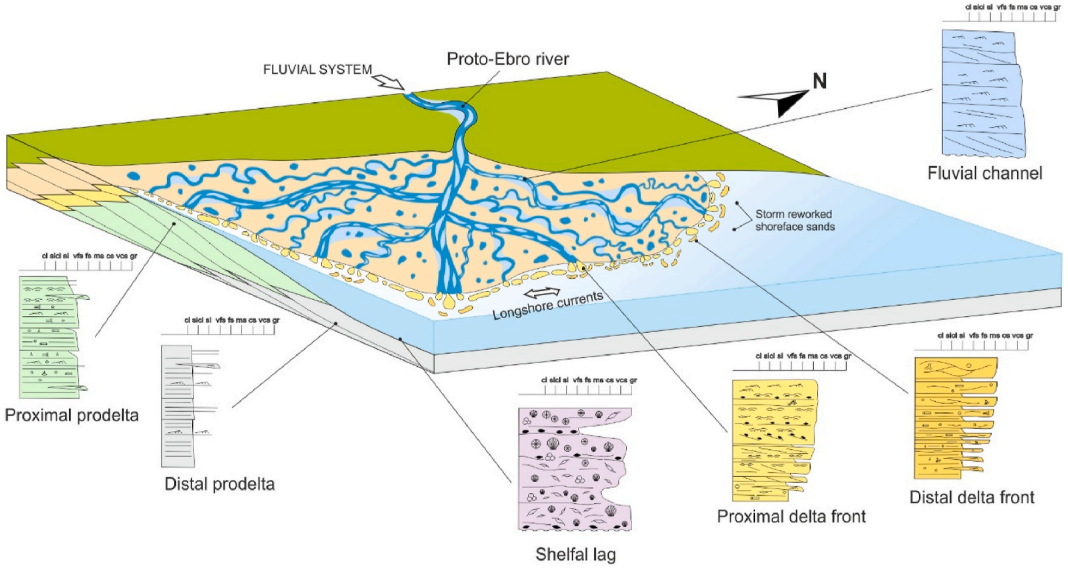

Fig. 11. Depositional model sketch for the Castellón Sandstones Formation, as the proto-Ebro delta during the Late Miocene in the Valencia Trough. See the river-processes are dominant in the overall architecture of the deltaic system, but also influenced and modelled by the action of waves. Not to scale.

lows could constitute an extra in storage capacity, as are regionally covered by the thick shaly section of the Ebro Shales Formation, although further work to quantify its capacity would be needed.

Given the broad extension of the Castellón Sandstones Formation and depth in which this succession is found in the area (>800m), it is presented as a good candidate for geological carbon storage in the study area, considering also its proximity to the onshore Tarragona's industrial complex. The regional lateral and vertical connectivity of delta front lobes and channels remains the main geological uncertainty for the development of a feasible CCS project. However, a preliminary correlation carried out in the zone has proved the lateral connectivity of delta front and delta plain facies belts in a reduced area around Castellón B wells (Fig. 10-D).

Our description of the cored section from Amposta Marino C-2 well shows that most of the facies associations are below the vertical resolution of the available seismic data and the fact that this study is based on the interpretation of a partial core from Amposta Marino C-2 well, is indeed a limitation of our work, highlighting the need for additional data from other wells to improve the geological model of the area.

Complementary analysis, such as, an accurate chronostratigraphic study of the whole Castellón Sandstones succession, would help to better correlate packages between wells and to create a 3D property model for a selected CO_2 storage site. However, the lack of core, sidewall core and image log data in most of the legacy wells in the study area poses a challenge for fine-correlation between wells. In that sense, a biostratigraphic analysis with cuttings would be highly recommended to lower uncertainty avoiding erroneous lithostratigraphic correlations in terms of vertical and lateral connectivity of geobodies. An accurate petrophysical and petrographic analysis would also be desirable to define reservoir zones linked to reservoir quality properties within the area.

The correlation between wells made in this study marks the first step on developing a potential 3D model for CCS. Some of the key surfaces to take into consideration have been identified as flooding surfaces and erosive surfaces. These flooding surfaces (FS1 to FS12) can be interpreted both, as product of relative sea level rises due to allocyclic processes, and/or as lateral avulsion of main delta front lobes during sedimentation due to autocyclic local changes in accommodation space and building of the delta complex. The erosive surfaces are regionally extended and could be related to relative sea level drops, interpreted as Regressive Surface of Marine Erosion (RSME, sensu Embry, 2009) perhaps associated with first episodes of the Mediterranean Sea closure before the Messinian Salinity Crisis, although this hypothesis would require further work to be confirmed.

6. Conclusions

The Castellón Sandstones Formation is mainly represented by a siliciclastic succession formed mainly by sandstones and sandy heterolithics in the Ebro Delta offshore area of the Valencia Trough. This succession has a maximum thickness around 850 m based on legacy wells in the study area. Eleven lithofacies, comprising sandstones, heterolithics, calcarenites and carbonate breccias, were identified on the cored section of Amposta Marino C-2 well, and grouped into six facies associations, including the following: 1) fluvial channel, 2) delta front proximal mouth bar, 3) delta front distal mouth bar, 4) proximal prodelta, 5) distal prodelta and 6) shelfal lag. The seismic stratigraphic analysis points out the presence of delta plain deposits in the northeastern sector of the BG_Ebro and Tortuga 3D seismic cubes, approximately 30 km away from the present-day Ebro delta shoreline. The interpretation of these facies and seismic facies associations allowed us to propose a depositional model of a river dominated, wave-influenced delta for the proto-Ebro deltaic system during the Late Miocene in the Valencia Trough. The sand-prone deposits of the delta front and fluvial channels interlayered with fine-grained delta plain and prodelta, present a high potential for permanent carbon sequestration in the subsurface in the area. Fine-grained prodelta deposits of the Ebro Shales Formation apparently may act as a regional seal for underlying sand-rich delta front and delta plain deposits of the Castellón Sandstones Formation.

CRediT authorship contribution statement

Marc Gil-Ortiz: Writing – review & editing, Writing – original draft, Methodology, Investigation, Formal analysis, Conceptualization. **Enrique Gomez-Rivas:** Writing – review & editing, Writing – original draft, Methodology, Investigation, Formal analysis, Conceptualization. **Juan Alcalde:** Writing – review & editing, Writing – original draft, Methodology, Investigation, Formal analysis, Conceptualization. **Patricia Cabello:** Writing – review & editing, Writing – original draft, Methodology, Investigation, Formal analysis, Conceptualization. **Luis Miguel Yeste:** Writing – review & editing, Writing – original draft, Methodology, Investigation, Formal analysis, Conceptualization. **Gonzalo Zamora:** Writing – review & editing, Writing – original draft, Methodology, Investigation, Formal analysis, Conceptualization. **Ángel Carrasco:** Writing – review & editing, Writing – original draft, Methodology, Investigation, Formal analysis, Conceptualization. **David García Fernández-Valderrama:** Writing – review & editing, Writing – original draft, Methodology, Investigation, Formal analysis, Conceptualization. **Antonio Martín-Monge:** Writing – review & editing, Writing – original draft, Methodology, Investigation, Formal analysis, Conceptualization. **Marta Mañas:** Writing – review & editing, Writing – original draft, Methodology, Investigation, Formal analysis, Conceptualization. **María Victoria Olgado Azpiazu:** Writing – review & editing, Writing – original draft, Methodology, Investigation, Formal analysis, Conceptualization. **Manuel Ron Martín:** Writing – review & editing, Writing – original draft, Methodology, Investigation, Formal analysis, Conceptualization. **Pujianto Lukito:** Writing – review & editing, Writing – original draft, Methodology, Investigation, Formal analysis, Conceptualization. **Francisco Pángaro:** Writing – review & editing, Writing – original draft, Methodology, Investigation, Formal analysis, Conceptualization.

Declaration of competing interest

The authors declare that they have no known competing financial interests or personal relationships that could have appeared to influence the work reported in this paper.

Acknowledgements

Special thanks are due to Repsol Exploración S.A. for funding the postdoctoral fellowship of Marc Gil-Ortiz as well as for technical support, data sharing and permission to publish this study. We acknowledge support from grant PID2020-118999 GB-I00 funded by MCIN/AEI/10.13039/501100011033, grants PID2022-140850OB-C21 and PID2022-140850OB-C22 funded by MICIU/AEI/10.13039/501100011033 and by "ERDF/EU", the "Consolidación Investigadora" grants CNS2023-145382 (to Enrique Gomez-Rivas) funded by MCIN/AEI/10.13039/50110001103 and European Union NextGenerationEU/PRTR, and projects 2021 SGR 00349 "Geologia Sedimentària" and 2021 SGR 00076 "Geodinàmica i Anàlisi de Conques" funded by AGAUR are gratefully acknowledged. Thanks to an anonymous reviewer and also to the editors of the *Marine and Petroleum Geology,* especially to Istvan Csato, for their constructive comments that have improved the content of this paper.

Data availability

The data that has been used is confidential.

References

Al-Khdheeawi, E.A., Vialle, S., Barifcani, A., Sarmadivaleh, M., Iglauer, S., 2017. Influence of injection well configuration and rock wettability on CO2 plume behaviour and CO2 trapping capacity in heterogeneous reservoirs. J. Nat. Gas Sci. Eng. 43, 190–206.

Al-Khdheeawi, E.A., Vialle, S., Barifcani, A., Sarmadivaleh, M., Iglauer, S., 2018. Enhancement of CO2 trapping efficiency in heterogeneous reservoirs by water-alternating gas injection. Greenhouse Gases: Sci. Technol. 8 (5), 920–931.

Alcalde, J., Heinemann, N., James, A., Bond, C.E., Ghanbari, S., Mackay, E.J., Haszeldine, R.S., Faulkner, D.R., Worden, R.H., Allen, M.J., 2021. A criteria-driven approach to the CO_2 storage site selection of East Mey for the acorn project in the North Sea. Mar. Petrol. Geol. 133, 105309. https://doi.org/10.1016/j.marpetgeo.2021.105309.

Álvarez-de-Buergo, E., Meléndez-Hevia, F., 1994. Características generales de las subcuencas del margen peninsular mediterráneo ("Rift" del Surco de Valencia). Acta Geol. Hisp. 29 (1), 67–79.

Ambrose, W.A., Lakshminarasimhan, S., Holtz, M.H., Núñez-López, V., Hovorka, S.D., Duncan, I., 2008. Geologic factors controlling CO2 storage capacity and permanence: case studies based on experience with heterogeneity in oil and gas reservoirs applied to CO2 storage. Environ. Geol. 54 (8), 1619–1633.

Arche, A., Evans, G., Clavell, E., 2010. Some considerations on the initiation of the present SE Ebro river dranaige system: Post- or pre-Messinian? J. Iber. Geol. 36 (1), 73–85.

Ayala, C., Torne, M., Roca, E., 2015. A review of the current knowledge of the crustal and lithospheric structure of the Valencia Trough Basin. Bol. Geol. Min. 126 (2–3), 533–552.

Bárbara, C.P., Cabello, P., Bouche, A., Aarnes, I., Gordillo, C., Ferrer, O., Roma, M., Arbués, P., 2019. Quantifying the impact of the structural uncertainty on the gross rock volume in the Lubina and Montanazo oil fields (Western Mediterranean). Solid Earth 10, 1597–1619. https://doi.org/10.5194/se-10-1597-2019.

Bertoni, C., Cartwright, J., 2005. 3D seismic analysis of slope-confined canyons from the Plio-Pleistocene of the Ebro Continental Margin (Western Mediterranean). Basin Res. 17, 43–62. https://doi.org/10.1111/j.1365-2117.2005.00254.x.

Bullock, L.A., Alcalde, J., Tornos, F., Fernandez-Turiel, J.-L., 2023. Geochemical carbon dioxide removal potential of Spain. Sci. Total Environ. 867, 161287. https://doi.org/10.1016/j.scitotenv.2022.161287.

Cabrera, Ll, Roca, E., Garcés, M., de Porta, J., 2004. Estratigrafía y evolución tectonosedimentaria oligocena superior-neógena del sector central del margen catalán (Cadena Costero-Catalana). In: Vera, J.A. (Ed.), Geología De España, Sociedad Geológica De España. Instituto Geológico y Minero de España, Madrid, Spain, pp. 569–572.

Cameselle, A.L., Urgeles, R., 2015. Large-scale margin collapse during Messinian early sea-level drawdown: the SW Valencia trough, NW Mediterranean. Basin Res. 29 (S1), 576–595.

Cameselle, A.L., Urgeles, R., De Mol, B., Camerlenghi, A., Canning, J.C., 2014. Late Miocene sedimentary architecture of the ebro Continental Margin (Western mediterranean): implications to the Messinian salinity crisis. Int. J. Earth Sci. 1–18.

Cattaneo, A., Steel, R.J., 2003. Transgressive deposits: a review of their variability. Earth Sci. Rev. 62, 187–228. https://doi.org/10.1016/S0012-8252(02)00134-4.

Chadwick, R., Zweigel, P., Gregersen, U., Kirby, G., Holloway, S., Johannessen, P., 2004. Geological reservoir characterization of a CO2 storage site: the Utsira Sand, Sleipner, northern North Sea. Energy (Calg.) 29, 1371–1381.

Clavell, E., 1992. Geologia Del Petroli De Les Conques Terciàries De Cataluña. University of Barcelona, Barcelona. Doctoral thesis.

Clavell, Berastegui, 1991. Petroleum geology of the Gulf of Valencia. In: Spencer, M.A. (Ed.), Generation, Accumulation, and Production of Europe's Hydrocarbons. Oxford University Press, Oxford, pp. 355–368. Special Publication of the European Association of Petroleum Geoscientists, 1.

Di Cuia, R., Riva, A., Ricciato, A., Marian, M., 2017. Valencia trough (Offshore Spain): petroleum systems and play types. AAPG search and discovery. In: AAPG 2017 Annual Convention & Exhibition. Houston, Texas, April 2-5, 2017.

Eigbe, P.A., Ajayi, O.O., Olakoyejo, O.T., Fadipe, O.L., Efe, S., Adelaja, A.O., 2023. A general review of CO_2 sequestration in underground geological formations and assessment of depleted hydrocarbon reservoirs in the Niger Delta. Appl. Energy 350, 121723. https://doi.org/10.1016/j.apenergy.2023.121723.

Embry, A., 2009. Practical Sequence Stratigraphy. Canadian Society of Petroleum Geologists, Canada, p. 79.

EMODnet - European Marine Observation and Data Network bathymetry portal, 2024. EMODnet map viewer. https://emodnet.ec.europa.eu/en. (Accessed 23 September 2024).

Escutia, C., Maldonado, A., 1992. Palaeogeographic implications of the Messinian surface in the Valencia trough, northwestern Mediterranean Sea. Tectonophysics 203, 263–284.

Evans, G., Arche, A., 2002. The flux of siliciclastic sediment from the Iberian Peninsula, with particular reference to the Ebro. In: Jones, S.J., Frostick, L.E. (Eds.), Sediment Flux to Basins: Causes, Controls and Consequences. Geol Soc Spec Publ, London, pp. 199–208.

Fang, P., Tugend, J., Mohn, G., Kusznir, N., Ding, W., 2021. Evidence for rapid large-amplitude vertical motions in the Valencia Trough (Western Mediterranean) generated by 3D subduction slab roll-back. Earth Planet Sci. Lett. 575, 117179. https://doi.org/10.1016/j.epsl.2021.117179.

Fernández-Canteli Álvarez, P., García Crespo, J., Martínez Orío, R., Mediato Arribas, J.F., Ramos, A., Berrezueta, E., 2023. Techno-economic evaluation of regional CCUS implementation: the STRATEGY CCUS project in the Ebro Basin (Spain). Greenhouse Gases: Sci. Technol. 13, 197–215. https://doi.org/10.1002/ghg.2193.

Frey-Martínez, J., Cartwright, J.A., Burgess, P.M., Vicente-Bravo, J., 2004. 3D seismic interpretation of the Messinian unconformity in the Valencia Basin, Spain. In: Davies, R.J., Cartwright, J.A., Stewart, S.A., Lappin, M., Underhill, J.R. (Eds.), 3D Seismic Technology: Application to the Exploration of Sedimentary Basins. Geological Society, London, Memoirs, pp. 91–100, 29.

García, M., Maillard, A., Aslanian, D., Rabineau, M., Alonso, B., Gorini, C., Estrada, F., 2011. The Catalan margin during the Messinian salinity crisis: physiography, morphology and sedimentary record. Mar. Geol. 284, 158–174. https://doi.org/10.1016/j.margeo.2011.03.017.

Garcia-Castellanos, D., Villaseñor, A., 2011. Messinian salinity crisis regulated by competing tectonics and erosion at the Gibraltar arc. Nature 480, 359–363. https://doi.org/10.1038/nature10651.

Garcia-Castellanos, D., Vergés, J., Gaspar-Escribano, J., Cloetingh, S., 2003. Interplay between tectonics, climate, and fluvial transport during the Cenozoic evolution of the Ebro Basin (NE Iberia). J. Geophys. Res. 108, 2347. https://doi.org/10.1029/2002JB002073.

Garcia-Castellanos, D., Estrada, F., Jiménez-Munt, I., Gorini, C., Fernández, M., Vergés, J., De Vicente, R., 2009. Catastrophic flood of the Mediterranean after the Messinian Salinity Crisis. Nature 462, 778–781. https://doi.org/10.1038/nature08555.

Garcia-Sineriz, B., Querol, R., Castillo, F., Fernández, J.R., 1978. A new hydrocarbon province in the Western Mediterranean. In: Proceedings of the 10th World Petroleum Congress, pp. 1–4.

Gershenzon, N.I., Ritzi, R.W., Dominic, D.F., Soltanian, M., Mehnert, E., Okwen, R.T., 2015. Influence of small-scale fluvial architecture on CO2 trapping processes in deep brine reservoirs. Water Resour. Res. 51, 8240–8256.

Gershenzon, N.I., Ritzi, R.W., Dominic, D.F., Mehnert, E., 2017. Effective constitutive relations for simulating CO2 capillary trapping in heterogeneous reservoirs with fluvial sedimentary architecture. Geomech. Geophys. Geo-Energy Geo-Res. 3, 265–279.

IEA, 2024. CO2 Emissions in 2023. A New Record High, but is there Light at the End of the Tunnel? International Energy Agency, p. 24.

Issautier, B., Viseur, S., Audigane, P., Le Nindre, Y.-M., 2014. Impacts of fluvial reservoir heterogeneity on connectivity: implications in estimating geological storage capacity for CO2. Int. J. Greenh. Gas Control 20, 333–349.

Issautier, B., Viseur, S., Audigane, P., Chiaberge, C., Le Nindre, Y.-M., 2016. A new approach for evaluating the impact of fluvial type heterogeneity in CO2 storage reservoir modeling. C. R. Geosci. 348, 531–539.

Kertznus, V., Kneller, B., 2009. Clinoform quantification for assessing the effects of external forcing on continental margin development. Basin Res. 21, 738–758. https://doi.org/10.1111/j.1365-2117.2009.00411.x.

Lanaja, J.M., 1987. Contribución de la exploración petrolífera al conocimiento de la geología de España. In: *Instituto Geológico Y Minero De España*. IGME. Serv. Publ. Industr. Energ., Madrid, p. 465.

Lofi, J., Sage, F., Déverchère, J., Loncke, L., Maillard, A., Gaullier, V., Thinon, I., Gillet, H., Guennoc, P., Gorini, C., 2011. Refining our knowledge of the Messinian salinity crisis records in the offshore domain through multi-site seismic analysis. Bull. Soc. Geol. Fr. 182, 163–180.

Maillard, A., Mauffret, A., 2006. Relationships between erosion surfaces and Late Miocene Salinity Crisis deposits in the Valencia Basin (northwestern Mediterranean): evidences for an early sea-level fall. Terra Nova 18, 321–329.

Maillard, A., Mauffret, A., Watts, A.B., Torné, M., Pascal, G., Buhl, P., Pinet, B., 1992. Tertiary sedimentary history and structure of the Valencia trough (western Mediterranean). Tectonophysics 203, 57–75.

Maillard, A., Gorini, C., Mauffret, A., Sage, F., Lofi, J., Gaullier, V., 2006. Offshore evidence of polyphase erosion in the Valencia Basin (Northwestern Mediterranean): scenario for the Messinian Salinity Crisis. Sediment. Geol. 188–189, 69–91.

Martín-Monge, A., Carrasco Castro, Á., Mañas Fernández, M., Lukito, P., Ron Martín, M., García Fernández-Valderrama, D., Pángaro, F., 2024. Seal assessment for the TarraCO2 geological carbon storage site, offshore ebro Delta. Geotemas (Madr.) 20, 1312.

Martínez del Olmo, W., 1996. Yesos de margen y turbidíticos en el Messiniense del Golfo de Valencia: una desecación imposible. Rev. Soc. Geol. de Esp. 9, 97–116.

Martínez del Olmo, W., 2011. El Messiniense en el Golfo de Valencia y el Mar de Alborán: Implicaciones paleogeográficas y paleoceanográficas. Rev. Soc. Geol. Espana 24, 3–4.

Martínez del Olmo, W., 2019. The Spanish petroleum systems and the overlooked areas and targets. Bol. Geol. Min. 130 (2), 289–315. https://doi.org/10.21701/bolgeomin.130.2.005.

Martínez del Olmo, W., 2021. Interpretación de secuencias deposicionales de 3er orden: aplicación a las sucesiones estratigráficas del Mesozoico del Prebético y del Neógeno del Golfo de Valencia. Bol. Geol. Min. 132 (3), 299–324. https://doi.org/10.21701/bolgeomin.132.3.004.

Martínez del Olmo, W., Martín, D., 2016. The Messinian record of Spanish onshore and offshore data (Atlantic Ocean and Western Mediterranean Sea). Pet. Geosci. 22, 291–296. https://doi.org/10.1144/petgeo2015-085.

Navarro Comet, J., 2019. Casablanca: spain's biggest oil field. *AAPG Explorer*, March 2019, Historical Highlights, pp. 20–23.

Pellen, R., Aslanian, D., Rabineau, M., Suc, J.P., Gorini, C., Leroux, E., Blanpied, C., Silenziario, C., Popescu, S.M., Rubino, J.L., 2019. The Messinian Ebro River incision. Global Planet. Change 181, 102988. https://doi.org/10.1016/j.gloplacha.2019.102988.

Permanyer, A., Marfil, R., de la Peña, J.A., Dorronsoro, C., Rossi, C., 1999. Potential petrolígeno de la formación Margas de Mas d'Ascla (Jurásico superior) en la Cuenca del Maestrazgo. Actas II Cong. Ibér. Geoquim. 199–202. Lisboa.

Pham, V.T.H., Halland, E.K., Tappel, I.M., Gjeldvik, I.T., Riis, F., Aagaard, P., 2013. Long-term behavior of CO2 stored on a large scale in the Utsira Formation, the North Sea, Norwegian Continental Shelf. Energy Proc. 37, 5240–5247.

Playà, E., Travé, A., Caja, M.A., Salas, R., Martín-Martín, J.D., 2010. Diagenesis of the Amposta offshore oil reservoir (Amposta Marino C2 well, Lower Cretaceous, Valencia Trough, Spain). Geofluids (Oxf.) 10, 314–333. https://doi.org/10.1111/j.1468-8123.2009.00266.x.

Roca, E., 1994. La evolución geodinámica de la Cuenca Catalano-Balear y áreas adyacentes desde el Mesozoico hasta la actualidad. Acta Geol. Hisp. 29, 3–25.

Roca, E., Guimerà, J., 1992. The Neogene structure of the eastern Iberian margin: structural constrains on the crustal evolution of the Valencia trough (western Mediterranean). Tectonophysics 203, 203–218.

Roca, E., Sans, M., Cabrera, L., Marzo, M., 1999. Oligocene to middle Miocene evolution of the central Catalan margin (northwestern Mediterraenan). Tectonophysics 315, 209–233.

Roca, E., Frizon de Lamotte, D., Mauffret, A., Bracène, R., Vergés, J., Benaouali, N., Fernández, M., Muñoz, J.A., Zeyen, H., 2004. TRANSMED transect II. In: Cavazza, W., Roure, F., Spakman, W., Stampfli, G.M., Ziegler, P. (Eds.), The TRANSMED Atlas-The Mediterranean Region from Crust to Mantle. Springer, Berlin.

Rossi, C., Goldstein, R.H., Marfil, R., Salas, R., Benito, M.I., Permanyer, A., de la Peña, J. A., Caja, M.A., 2001. Diagenetic and oil migration history of the Kimmeridgian Ascla Formation, Maestrat Basin, Spain. Mar. Petrol. Geol. 18, 287–306.

Sàbat, F., Roca, E., Muñoz, J.A., Vergés, J., Santanach, P., Sans, M., Masana, E., Estévez, A., Santisteban, C., 1997. Role of extension and compression in the evolution of the eastern margin of Iberia: the ESCI-València Trough seismic profile. Rev. Soc. Geol. Esp. 8, 431–448.

Salas, R., 1989. Evolución estratigráfica secuencial y tipos de plataformas de carbonatos del intervalo Oxfordiense–Berriasiense en las cordilleras Ibérica oriental y costerocatalana meridional. Cuad. Geol. Iber. 13, 121–157.

Salas, R., Permanyer, A., 2003. Evidencias de generación de hidrocarburos en la formación de margas del Mas d'Ascla (Jurásico superior, Cadena Ibérica oriental) y su relación con el campo de Amposta de la Cuenca de Tarragona. Bol. Geol. Min. 114, 75–86.

Soler, R., Martinez del Olmo, W., Megias, A.G., Abeger-Monteagudo, J.A., 1983. Rasgos básicos del Neógeno del Mediterráneo Español. Mediterr. - Ser. Estud. Geol. 1, 71–82.

Soltanian, M.R., Hajirezaie, S., Hosseini, S.A., Dashtian, H., Amooie, M.A., Meyal, A., Ershadnia, R., Ampomah, W., Islam, A., Zhang, X., 2019. Multicomponent reactive transport of carbon dioxide in fluvial heterogeneous aquifers. J. Nat. Gas Sci. Eng. 65, 212–223.

Stampfli, G.M., Höcker, C.F.W., 1989. Messinian palaeorelief from a 3-D seismic survey in the Tarraco concession area (Spanish Mediterranean Sea). Geol. Mijnbouw 68, 201–210.

Sun, X., Alcalde, J., Bakhtbidar, M., Elío, J., Vilarrasa, V., Canal, J., Ballesteros, J., Heinemann, N., Haszeldine, S., Cavanagh, A., Vega-Maza, D., Rubiera, F., Martínez-Orio, R., Johnson, G., Carbonell, R., Marzan, I., Travé, A., Gomez-Rivas, E., 2021. Hubs and clusters approach to unlock the development of carbon capture and storage – case study in Spain. Appl. Energy 300, 117418.

Tassy, A., Fournier, F., Munch, P., Borgomano, J., Thinon, I., Fabri, M.-C., Rabineau, M., Arfib, B., Begot, J., Beslier, M.-O., Cornée, J.-J., Fournillon, A., Gorini, C., Guennoc, P., Léonide, P., Oudet, J., Paquet, F., Sage, F., Toullec, R., 2014. Discovery of Messinian canyons and new seismic stratigraphic model, offshore Provence (SE France): implications for the hydrographic network reconstruction. Mar. Petrol. Geol. 57, 25–50. https://doi.org/10.1016/j.marpetgeo.2014.05.001.

Urgeles, R., Camerlenghi, A., Garcia-Castellanos, D., De Mol, B., Garcés, M., Vergés, J., Haslam, I., Hardman, M., 2011. New constraints on the Messinian sealevel drawdown from 3D seismic data of the Ebro Margin, western Mediterranean. Basin Res. 23, 123–145.

Williams, G.A., Chadwick, R.A., 2021. Influence of reservoir-sclae heterogeneities on the growth, evolution and migration of a CO2 plume at the Sleipner Field, Norwegian North Sea. Int. J. Greenh. Gas Control 106, 103260. https://doi.org/10.1016/j.ijggc.2021.103260.

Zweigel, P., Arts, R., Lothe, A.E., Lindeberg, E.B.G., 2004. Reservoir Geology of the Utsira Formation at the First industrial-scale Underground CO2 Storage Site (Sleipner Area, North Sea), vol. 233. Geological Society of London, Special Publication, pp. 165–180.